Environmental and economic assessment of lactic acid production from glycerol using cascade bio- and chemocatalysis

Journal Article

Author(s):
Morales, Merten; Dapsens, Pierre Y.; Giovinazzo, Isabella; Witte, Julia; Mondelli, Cecilia; Papadokonstantakis, Stavros; Hungerbühler, Konrad; Pérez-Ramírez, Javier

REPORT

Environmental and economic assessment of lactic acid production from glycerol using cascade bio- and chemocatalysis

Merten Morales,‡ Pierre Y. Dapsens,‡ Isabella Giovinazzo, Julia Witte, Cecilia Mondelli*, Stavros Papadokonstantakis*, Konrad Hungerbühler and Javier Pérez-Ramírez*

Recently, lactic acid has emerged as one of the most relevant platform molecules for the preparation of bio-chemicals. Due to the limited productivity of sugar fermentation, the dominant industrial technology practiced for its manufacture, new chemocatalytic processes are being developed in order to meet the
10 expected demand for this intermediate. The Lewis-acid catalysed isomerisation of dihydroxyacetone has attracted particular interest. If the reaction is performed in water, lactic acid is attained directly, while if alcohols are used as the solvent the desired product can be obtained upon subsequent hydrolysis of the alkyl lactates formed. Herein, we (*i*) demonstrate tin-containing MFI zeolites prepared by scalable methods as highly active, selective and recyclable catalysts able to operate in concentrated
15 dihydroxyacetone aqueous and methanolic solutions, and (*ii*) reveal by life cycle analysis that a process comprising the enzymatic production of dihydroxyacetone from crude glycerol and its chemocatalytic isomerisation in methanol is advantageous for the production of lactic acid compared to glucose fermentation in terms of both sustainability and operating costs. In particular, we demonstrate that the reduced energy requirements and CO_2 emissions of the cascade process originate from the valorisation of
20 a waste feedstock and from the high performance and recyclability of the zeolite catalyst and that the economic advantage is strongly determined by the comparably low market price of glycerol. It is also shown that the bio-/chemocatalytic route remains ecologically and economically more attractive even if the purity of glycerol is as low as 38%.

1 Introduction

25 In the last years, many research efforts have been directed to the conversion of bio-derived feedstocks into chemicals as a means to address the forthcoming oil shortage, mitigate global warming and meet the consumers' demand for greener products.[1] In this context, lactic acid (LA) has gained significant interest.[2] This
30 compound not only can generate multiple commodity and intermediate chemicals (*e.g.*, acrylic acid, 1,2-propanediol, pyruvic acid, acetaldehyde, 2,3-pentanedione) that already belong to our traditional chemistry portfolio, but it can also be polymerised into a novel biodegradable plastic suitable for
35 packagings, *i.e.*, polylactide (PLA). This polymer was already industrially produced in an amount of 180 kton in 2012 and its manufacture is projected to reach 1 Mton year⁻¹ by 2020. This value might even be exceeded considering that PLA could replace PET (58 Mton in 2012) in 20% of its current
40 applications.[2,3]

Nowadays, LA is prepared *via* the anaerobic batch fermentation of glucose (GLU) or sucrose, under strict temperature (< 313 K) and pH (5-7) conditions, followed by

purification through subsequent esterification, distillation and
45 hydrolysis (Scheme 1).[4] One prominent environmental issue related to this manufacturing method is the coproduction of large amounts of gypsum (1 ton per 1 ton of LA), which has to be disposed. Moreover, as typical of biocatalysis, the low productivity (1-13 g_{LA} L⁻¹ h⁻¹) of the process may be a high
50 hurdle for the expansion of this technology to fulfil the future demand for LA.[4] Accordingly, alternative pathways based on chemocatalysis have been explored,[5] such as the aqueous-phase isomerisation of 1,3-dihydroxyacetone (DHA) over Lewis acids.[2] Lanthanum and lead salts have proved highly active for
55 this reaction, even enabling the one-pot production of LA from cellulose.[5] Still, owing to their complex and energy-demanding separation from the reaction mixture as well as their toxicity, solid catalysts have attracted more pronounced interest (Scheme 1).[6] So far, research studies have been mainly devoted
60 to the identification of active and selective materials .[7] In this respect, Sn-containing BEA and MWW zeolites stand as the best performers, yielding > 96% LA.[6,8] The surprisingly lower LA yields over Sn-MFI zeolites is likely due to the suboptimal reaction conditions applied in their evaluation.[9] The LA yield
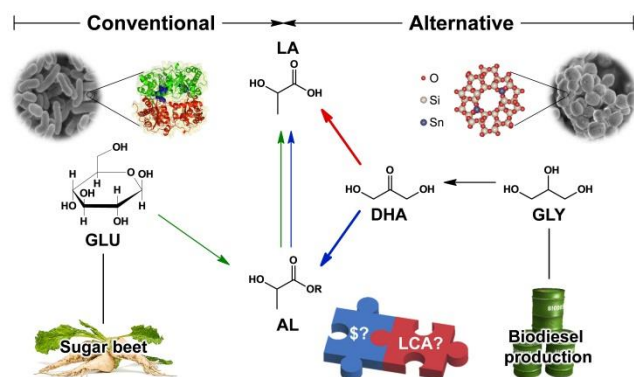
Scheme 1 Conventional lactic acid (LA) production *via* glucose (GLU) fermentation *versus* an alternative hybrid bio-/chemocatalytic route based on the enzymatic oxidation of glycerol (GLY) to 1,3-dihydroxyacetone (DHA) followed by isomerisation in water or in methanol *via* an alkyl lactate (AL) intermediate. Thick and thin arrows define the reactions for which experimental data have been derived from this work and from the literature, respectively.

over Al-based Lewis-acid solids has reached a maximum of 82% over alkaline-treated MFI zeolites.[10] In spite of these promising results, other critical aspects at the catalyst and process levels have been infrequently investigated in view of a potential large-scale application of this route.

At the *catalyst* level, crucial parameters are the scalability of the synthesis, the stability upon reaction and the ability to process concentrated feeds. In this context, dealumination of beta followed by solid- or liquid-phase tin incorporation has been introduced as a less demanding strategy than the complex and long hydrothermal synthesis to prepare Sn-BEA.[11] The method to produce Sn-MWW, comprising deboronation of hydrothermally-synthesised B-MWW and subsequent tin incorporation, features a comparable degree of complexity.[8] Hydrothermally-synthesised Sn-MFI and alkaline-treated MFI hold the brightest prospects as industrially-amenable catalysts. Indeed, the analogously prepared TS-1 zeolite has been manufactured by EniChem for nearly three decades for use in phenol hydroxylation [12] and desilication of commercial ZSM-5 has already been demonstrated at the pilot scale.[13] Concerning catalyst robustness, Sn-MWW has been shown to retain its performance in three consecutive catalytic runs, while hydrothermally-prepared Sn-BEA and alkaline-treated MFI to suffer from poor recyclability due to metal leaching.[8,10] The reusability of Sn-MFI has not been evaluated. The replacement of the aqueous medium by an alcoholic solvent has proved effective in preventing deactivation. Thus, the production of alkyl lactates (AL), relevant green solvents and chemical intermediates, by one-pot DHA isomerisation-esterification has been often preferred.[7,11a] In relation to LA productivity, no attempts have been made to verify that these zeolites could retain their outstanding activity and selectivity when applying higher DHA concentrations than 3 wt.% in the starting solution.

At the *process* level, critical aspects in determining economic and environmental performance are the number of unit operations, the reaction conditions (temperature, pressure, solvent), the types of separation methods and the cost, availability and cradle-to-gate life cycle impact of raw materials and chemical auxiliaries. Only some of these aspects have been addressed and

on an individual basis. For instance, in view of eliminating a separation step, it has been attempted to combine the production and isomerisation of DHA. Thus, Sn-BEA and Sn-MWW have been used in water or alcohols to isomerise GLU, cleave the generated fructose by a retro-aldol reaction and further convert the obtained DHA to LA/AL, while noble metals supported on oxides or (tin-containing) zeolites have been employed to oxidise glycerol (GLY) and isomerise DHA in one pot.[8,14] Still, even substantially reduced product yields have been attained compared to the one-step transformation and catalyst stability issues have emerged, thus questioning the advantage of these intensified processes. With respect to the bio-derived feedstock used, GLY has been regarded as a preferable source of DHA compared to sugars as it is an abundant waste (125 Mton expected in 2016) of biofuels production.[15] Furthermore, it can be enzymatically oxidised to the desired triose with very high yields (97% after 30 h of reaction) under acidic pH conditions, avoiding the generation of gypsum waste streams.[16] Based on these observations, it is clear that a quantitative assessment of the economic profitability and environmental sustainability of the new value chains for LA production would be extremely relevant in order to adequately define their industrial potential.[17] In this respect, evaluating the relative impact of variables such as catalyst stability and number of production steps is particularly important. Indeed, LA could be also recovered from alkyl lactates, whose production undermines the integrity of the Lewis-acid solids to a lower extent, through an additional hydrolysis step in water, in analogy to the biocatalytic route (Scheme 1)**.**

Herein, we first evaluate the performance and the reusability of Sn-containing MFI zeolites in the isomerisation of concentrated (15 wt.%) DHA aqueous and methanolic solutions. We then perform rigorous process modelling and flowsheeting for a hybrid bio-/chemocatalytic route comprising enzymatic GLY oxidation and water- or alcohol-based DHA isomerisation and for the biochemical pathway to contrast the alternative approach to the current industrially-practiced technology. For this purpose, we combine the experimental results herein gathered on DHA isomerisation with available data for the fermentation of GLY to the ketonic triose and of sugar beet-derived GLU to LA. The comparison is made on the basis of economic and ecological metrics following a systematic life cycle assessment (LCA) methodology.[17]

2 Materials and methods

2.1 Experimental

Catalyst synthesis and characterisation

The Sn-containing MFI zeolites investigated in this study comprise Sn-MFI and MFI-ATSn. The former was prepared by hydrothermal synthesis in hydroxide medium and the latter by post-synthetic alkaline-assisted stannation of silicalite-1, according to reported procedures.[18,19] The catalysts were characterised in terms of porous and acidic properties, crystallinity, and tin and carbon content prior to and after use in the catalytic tests. A detailed description of the synthetic protocols and of the characterisation methods is available in the Electronic Supplementary Information (ESI).

Catalyst testing

Batch catalytic tests were performed under autogenous pressure in 100-cm³ thick-walled glass vials (Ace, pressure tubes, front seal) dipped in an oil bath heated at 413 K. The vials were loaded
5 with 7.6 g of DHA (Sigma-Aldrich, 98%, dimer), 4.12 g of catalyst and 40 g of solvent. The latter comprised deionised water or methanol (Scharlau, 99.9%). The mixture was allowed to react under vigorous stirring during 0.5 to 3 h. Thereafter, the reaction was quenched using an ice bath and the catalyst removed by
10 filtration under reduced pressure using cellulose acetate filters (Satorius, 0.45 μm). Reusability tests in water and methanol were performed for 1 h under the same conditions. Prior to every reuse, the catalyst was calcined in static air at 823 K (5 K min⁻¹) for 5 h. Continuous-flow experiments were conducted using a homemade
15 continuous-flow reactor setup composed of (*i*) an HPLC pump, (*ii*) a stainless-steel tubular reactor (Swagelok SS-T4-S-035, o.d. = ¼ inch, i.d. = 4.6 mm) heated by an oven and (*iii*) a backpressure regulator (Swagelok, LH2981001). The reactor was loaded with Sn-MFI (0.825 g) diluted with quartz (1.0 g, sieve
20 fraction = 0.25-0.36 mm) and heated at 403-413 K. Thereafter, the reaction was started by admitting a solution comprising 5 wt.% DHA in methanol at a rate of 0.2 cm³ min⁻¹. To prevent solvent loss by evaporation, the system was pressurised to 25 bar prior to heating. Samples were periodically collected from the
25 outlet stream for analysis.

DHA and LA were isolated by high-performance liquid chromatography (HPLC) in a Merck LaChrom system equipped with a Biorad Aminex HPX-87H column heated at 308 K and a refractive index detector (Hitachi Chromaster model 5450) set at
30 303 K, using an aqueous eluent of 0.005 M H_2SO_4 (pH = 2.30) flowing at 0.6 cm³ min⁻¹. Quantification was obtained by integration of their respective peaks. Methyl lactate (ML) was analysed using a gas chromatograph (HP 6890) equipped with an HP-5 capillary column and a flame ionisation detector. He was
35 used as the carrier gas (flow rate = 4.3 cm³ min⁻¹, pressure = 1.4 bar) and an injection volume of 0.2 μL was applied. The initial temperature of 328 K was held for 2 min before heating to 473 K (30 K min⁻¹). ML (Acros, 99%) was used as a reference and isooctane (Fluka, 99.5%) as a standard, which
40 was added to the reaction mixture after catalyst removal. The DHA conversion was calculated as the mole of DHA reacted divided by the mole of DHA fed, whereas the LA/ML yields as the mole of LA/ML formed divided by the initial moles of DHA.

2.2 Process modelling

45 Rigorous process models were developed for racemic LA production based on the routes depicted in Scheme 1. The. simulation software Aspen Plus® V8.2 was used for this purpose An overview of the models is presented in Table 1. In all cases, the main reactor units operate in batch mode, while the
50 downstream purification units in steady-state continuous mode. For sake of clarity, the intermediate storage tanks, facilitating the connection between the batch and the continuous part, were not represented. The process waste streams are treated in conventional industrial waste water treatment plants or
55 incineration units depending on their composition.[20] The basic features and respective flowsheets of each process model are described in the following sections whereas detailed information

Table 1 Overview of the process models developed for LA production

Model description	Acronym
Biocatalytic DHA production from pure GLY (99.99 wt.%)	*DHA-1*
Biocatalytic DHA production from crude GLY destined for the incineration plant*ᵃ*	*DHA-2*
Biocatalytic DHA production from crude GLY destined for the waste water treatment plant*ᵃ*	*DHA-3*
Biocatalytic DHA production from crude glycerol according to *DHA-3* followed by chemocatalytic LA production from DHA using the MFI-AT catalyst (3 consecutive runs) in water	*LA-1*
Biocatalytic DHA production from crude glycerol according to *DHA-3* followed by chemocatalytic LA production from DHA using the Sn-MFI catalyst (3 consecutive runs) in water	*LA-2*
Biocatalytic DHA production from crude glycerol according to *DHA-3* followed by chemocatalytic LA production from DHA using the Sn-MFI catalyst (7 consecutive runs) in water	*LA-3*
Biocatalytic DHA production from crude glycerol according to *DHA-3* followed by chemocatalytic LA production from DHA using the Sn-MFI catalyst (7 consecutive runs) in methanol	*LA-4*
Industrially applied biocatalytic LA production from GLU	*LA-5*

ᵃ The DHA-2 and DHA-3 models are identical, except for the distinct fate
60 that crude GLY would follow if it was not used as a chemical feedstock.

about the process conditions, amount of raw materials and of chemical auxiliaries, reaction conversions, production yields and separation procedures is available in the ESI.

Conventional LA production

65 This method is used by 90% of the LA producing companies, such as Cargill Inc. and Purac Biochem BV.[21] The process comprises five main steps: (*i*) the enzymatic generation of racemic LA from GLU with LA bacteria and its progressive neutralisation with $Ca(OH)_2$, (*ii*) the H_2SO_4-catalysed hydrolysis
70 of the calcium lactate formed, (*iii*) LA esterification with methanol, (*iv*) the purification of the obtained ML by distillation and finally, (*v*) ML hydrolysis to LA with water.[22] The flowsheet of the *LA-5* process model is shown in Fig. S3 in the ESI.

75 ### Alternative LA production from GLY

With respect to the alternative production of LA by chemocatalytic isomerisation of DHA, it was necessary to create a process model for the production of DHA, since its price (*ca.* 4500 USD ton⁻¹) is significantly higher than that of LA (1700-
80 2100 USD ton⁻¹) and the LA market has a greater volume than that of DHA.[23,24] As mentioned in the introduction, GLY fermentation was selected as the production method of the triose substrate.[25] The process comprises the following main steps: (*i*) fermentation of GLY (*ca.* 10 wt.% in water), (*ii*) concentration of
85 the reaction mixture and crystallisation of DHA out of butanol and (*iii*) recovery of butanol from the water-containing mother liquor through heterogeneous azeotropic distillation. Two process models were developed using pure GLY (99.99 wt.%, *DHA-1*) and crude GLY (75.8 wt.%, *DHA-2,3*). The composition of the
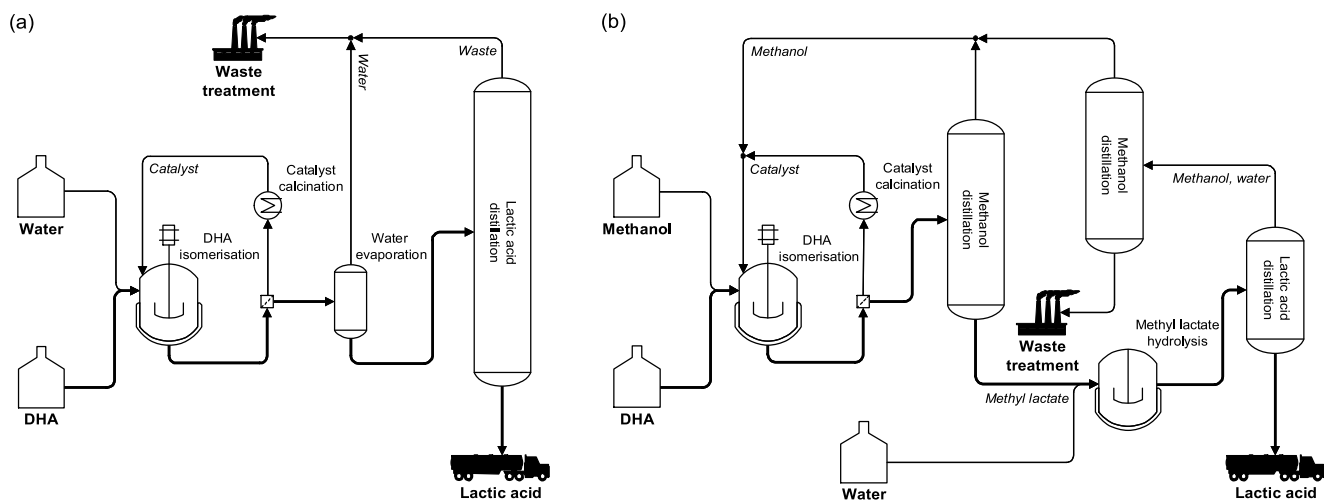
latter was derived from the study by Hansen *et al.*[26] Impurities comprise ash (5.3 wt.%), water (6.0 wt.%), matter organic non glycerol (MONG, 9.6 wt.%) and methanol (3.3 wt.%). The *DHA-2,3* models differ from the *DHA-1* model with respect to the additional treatment of crude GLY in order to remove ash, methanol and MONG prior to the fermentation. Their flowsheet is shown in Fig. 1 and the relative life cycle inventory (LCI) data are compiled in Table 2.

The product stream of the DHA manufacture was directed into the LA production process, which was conducted using either a Lewis-acid zeolite prepared by alkaline-treatment of a commercial Al-containing MFI sample (denoted as MFI-AT) or Sn-MFI. The performance (*i.e.*, productivity, recyclability, *etc.*) of the former catalyst is discussed in detail in [10] and that of the latter material in Section 3.1. Two process models were developed for racemic LA production over the two catalysts, which are based on: (*i*) the catalytic conversion of DHA to LA in water with acetol and pyruvic acid as the main by-products, (*ii*) the recovery of the catalyst by filtration and regeneration *via* calcination and *(iii-a)* the removal of impurities through distillations and crystallisation with butanol and the recovery of unreacted DHA for the process using MFI-AT or (*iii-b*) the concentration of the reaction mixture and the recovery of LA through vacuum distillation for the process using Sn-MFI. The different downstream work-up procedures originate from the distinct degree of conversion of DHA, which is partial over MFI-AT and full over Sn-MFI. The flowsheets for these processes are shown in Fig. S4 in the ESI (MFI-AT) and Fig. 2a (Sn-MFI) while the LCI data are compiled in Table 3 for both scenarios. The consumption of DHA is similar in either process as DHA is recovered if unconverted.

Replacing water with methanol in the Sn-MFI catalysed isomerisation resulted in some process flowsheet modifications. As DHA is fully transformed into ML generating negligible amounts of soluble by-products (see Section 3.1), ML and the excess of methanol can be recovered by distillation. ML is then

hydrolysed *via* a low-pressure reactive distillation producing pure LA and a mixture of methanol and water, which is further separated by conventional distillation to recover the organic fraction. The choice of methanol instead of ethanol or butanol as alcoholic medium was mainly based on this last distillation step, which would be azeotropic instead of conventional when using the C_2 and C_4 alcohols. The respective process flowsheet is shown in Fig. 2b and the associated LCI data are presented in

Table 2 LCI data for the biocatalytic production of DHA from GLY

Materials and energy	*DHA-2,3*	Units
Crude glycerol	1.5	kg kg_{DHA}^{-1}
Process water	10.2	kg kg_{DHA}^{-1}
Catalyst	–	kg kg_{DHA}^{-1}
Nutrients	0.05	kg kg_{DHA}^{-1}
Air	3.1	kg kg_{DHA}^{-1}
Butanol	0.06	kg kg_{DHA}^{-1}
Steam (6 bar)	44.7	MJ kg_{DHA}^{-1}
Cooling water	818	kg kg_{DHA}^{-1}
Waste	11.0	kg kg_{DHA}^{-1}

Table 3 LCI data for the chemocatalytic production of LA from DHA in water

Materials and energy	MFI-AT, 3[a]	Sn-MFI, 7[a]	Units
DHA	1.1	1.2	kg kg_{LA}^{-1}
Process water	6.5	5.8	kg kg_{LA}^{-1}
Butanol	0.02	-	kg kg_{LA}^{-1}
Catalyst	0.3	0.1	kg kg_{LA}^{-1}
Steam (6 bar)	18.2	13.7	MJ kg_{LA}^{-1}
Cooling water	434	271	kg kg_{LA}^{-1}
Waste	6.9	6.1	kg kg_{LA}^{-1}

[a] 3 and 7 indicate the number of cycles in which the catalyst was reused without loss in performance.

Fig. 1 Flowsheet for the DHA production process from crude glycerol according to the *DHA-2,3* models.

Fig. 2 Flowsheet for the chemocatalytic LA production process from DHA using the Sn-MFI catalyst in (a) water and (b) methanol.

5

Table 4 LCI data for the chemocatalytic production of LA from DHA in methanol

LCI data	Sn-MFI, 7[a]	Units
DHA	1.09	kg kg_{LA}^{-1}
Process water	0.41	kg kg_{LA}^{-1}
Methanol	0.03	kg kg_{LA}^{-1}
Catalyst	0.10	kg kg_{LA}^{-1}
Steam (6 bar)	12.7	MJ kg_{LA}^{-1}
Cooling water	649	kg kg_{LA}^{-1}
Waste	0.59	kg kg_{LA}^{-1}

[a] 7 corresponds to the number of cycles in which the catalyst was reused without loss in performance.

10 Table 4. Because of the recycling of methanol, less waste is generated but a higher cooling utility consumption is required compared to the process using MFI-AT in water. DHA, catalyst and steam consumption are equivalent in the LA production scenarios using Sn-MFI in water or methanol.

15 **2.3 Environmental and economic assessment**

The goal and scope of the environmental assessment following the LCA methodology is the comparison of the alternative process options presented in Scheme 1 for the production of 1 kg of LA. The process models were used for estimating the relevant 20 LCI data (*i.e.*, consumption of resources and process emissions) in a cradle-to-gate approach. The respective environmental impacts in the use phase and the environmental fate of LA after its use were not considered here (*i.e.*, no cradle-to-grave impacts were calculated). The materials for the plant construction were 25 also not included. Three well-known LCA metrics were followed, *i.e.*, the cumulative energy demand (CED), the global warming potential (GWP-100a) and the eco-indicator 99 (EI99). These metrics have been reported in previous chemical process assessment studies to cover different aspects of the environmental 30 impacts.[27] In the case of CED, we calculated here the non-renewable CED to focus on the depletion aspect for resource protection, which is the main motivation for a bio-based

production. A more detailed discussion on this topic can be found elsewhere.[28]

35 For the allocation of environmental impacts to crude GLY as a co-product of the biodiesel production, the approach and assumptions proposed by Weidema *et al* were followed.[29] Thus, crude GLY was considered as a partially utilised co-product from a consequential LCA perspective. Therefore, the 40 respective LCA metrics calculated in this study are valid as long as the amount of GLY employed in LA production is not restricted by the biodiesel production. In the case of pure GLY, the values allocated in the Ecoinvent database were used.[30] Due to the lack of literature data, the impact of the separation of 45 MONG *via* an acidulation process [31] on the LCA assessment was not considered.

The economic assessment was only based on operating costs. Investment costs are outside of the scope of the present study, since the production plants were not optimised for a specific 50 capacity. Although no capital cost estimations are provided, all flowsheets have similar LA productivity. All background data for the environmental and economic assessment are provided in the ESI.

3 Results and discussion

55 **3.1 Tin zeolites for LA production**

The Sn-containing zeolites prepared for LA production have a rather similar tin content (1.2 and 1.6 wt.% for Sn-MFI and MFI-ATSn, respectively). Their mesoporous surface is also comparable (Table 4), but, owing to the different preparation 60 procedures, the hydrothermally-synthesised zeolite is exclusively microporous while the solid obtained by alkaline-assisted stannation also features intracrystalline mesopores.[30,2] Additionally, the structural characteristics and placement of the catalytic tin centres in the samples are distinct, *i.e.*, tin is fully 65 integrated in the framework and uniformly distributed in the whole volume in the former, while it is totally or partially incorporated in the framework and predominantly at the external surface of the crystals in the latter.[32]

These materials were evaluated in DHA (15 wt.%) isomerisation at 413 K in water and methanol. Based on the kinetic profiles collected, the LA yield rapidly augmented with time attaining 85% at 97% DHA conversion for Sn-MFI (Fig. 3a) and 75% at 95% DHA conversion for MFI-ATSn (Fig. 3b) after only 30 min. Increasing the reaction time to 1 h enabled to convert the remaining DHA as well as the glyceraldehyde and pyruvaldehyde intermediates to the desired product, thus reaching LA yields of nearly 100% for both catalysts. LA was stable in the reaction mixture since its concentration remained unaltered for longer reaction times. Equivalent profiles were observed for the methanol-based isomerisation, the 1-h ML yield being only slightly lower for MFI-ATSn (*ca*. 93%) compared to Sn-MFI (*ca*. 98%) (Fig. 3c,d). The outstanding performance of Sn-MFI compared to previous reports [7b,9] indicates that optimal conditions were applied to the DHA isomerisation reaction. The similar catalytic behaviour of the stannated zeolite catalyst suggests that, as observed for the diffusion-free glyoxal substrate,[15,8] the advantage of a greater accessibility of tin sites compared to the hydrothermally-prepared sample is counterbalanced by the negative impact of their moderate structural heterogeneity. Investigation of the used catalysts by N_2 sorption and CHN analysis (Table 4) revealed substantial depletion of the porous volume due to the deposition of carbon-containing species (6 and 3 wt.% C on either catalysts in water and methanol, in the order). Accordingly, upon evaluating the stability of the solids in repeated 1-h runs, a calcination step was introduced prior to each reuse. For sake of clarity, Fig. 4 only displays the results of the first, second and last test (the complete set of data can be found in Fig. S1 in the ESI). The catalytic
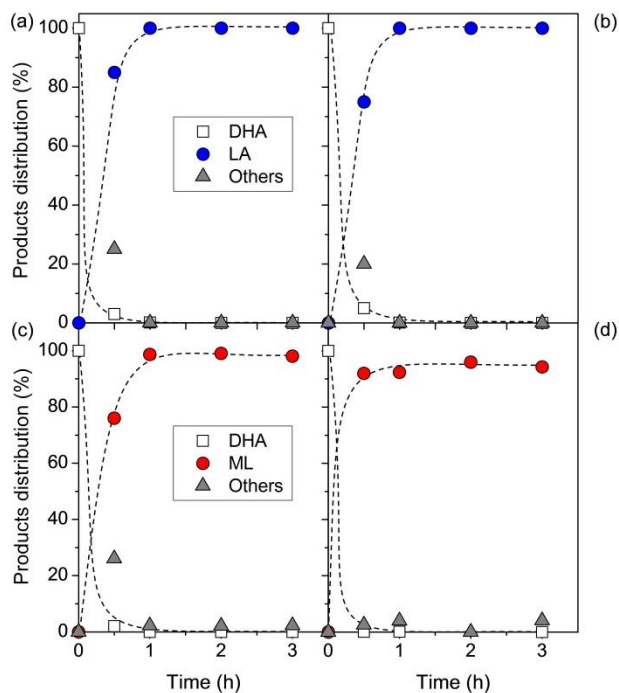
Fig. 3 Concentration profiles of reactant and products during the conversion of 15 wt.% DHA at 413 K over (a) Sn-MFI and (b) MFI-ATSn in water and over (c) Sn-MFI and (d) MFI-ATSn in methanol. "Others" include glyceraldehyde and pyruvaldehyde as well as acetic acid or pyruvaldehyde dimethyl acetal for the reaction in water or methanol, respectively.
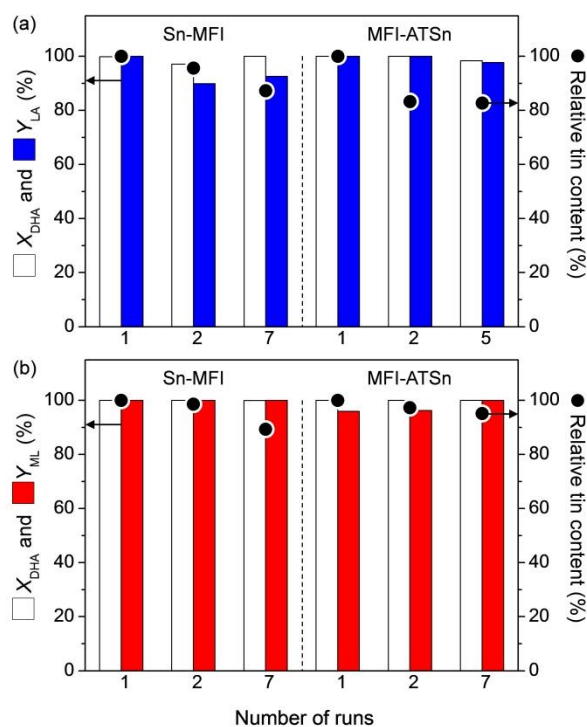
Fig. 4 Reusability tests for Sn-MFI and MFI-ATSn in (a) water and (b) methanol. The white bars refer to the DHA conversion while the blue/green bars identify the LA/ML yields.

Table 4 Porous properties of fresh, used and regenerated zeolite catalysts

Catalyst	State	$S_{meso}{}^a$ ($m^2\ g^{-1}$)	$V_{micro}{}^a$ ($cm^3\ g^{-1}$)	$V_{pore}{}^b$ ($cm^3\ g^{-1}$)
Sn-MFI	Fresh	49	0.17	0.24
	Used, H_2O	87	0.11	0.27
	Reg., H_2O	47	0.16	0.26
	Used, MeOH	39	0.12	0.23
	Reg., MeOH	52	0.16	0.28
MFI-ATSn	Fresh	50	0.11	0.22
	Used, H_2O	77	0.13	0.27
	Reg., H_2O	101	0.12	0.27
	Used, MeOH	62	0.11	0.22
	Reg., MeOH	63	0.13	0.25

^{a} Determined by the *t*-plot method. ^{b} Volume adsorbed at $p/p_0 = 0.99$.

performance of Sn-MFI was unaltered in methanol, while a slight deactivation was observed in water. A similar behaviour was observed for MFI-ATSn. Average LA yields of 93 and 99% and ML yields of 98 and 97% at full DHA conversion were determined for the hydrothermally-synthesised and the stannated samples, respectively. As indicated by the reduced tin content and amount of Lewis-acid sites (measured by elemental analysis and infrared spectroscopy of adsorbed pyridine, respectively) and by the retained crystallinity (determined by X-ray diffraction) of the recycled materials, the activity loss was related to metal leaching (Fig. 4 and Fig. S2 in the ESI). As mentioned above, this phenomenon has been reported as the main cause of deactivation of catalysts in DHA isomerisation, usually being more pronounced in aqueous than in alcoholic media. Even if very moderate and undetrimental for the catalyst recyclability, our results follow the same trend (*i.e.*, −10 and 17 % in water and −3 and 10% in methanol for Sn-MFI and MFI-ATSn, respectively).

The origin of tin leaching has not been elucidated at a molecular level so far. Nevertheless, the stability of tin-containing MFI zeolites in the isomerisation of glyoxal in water and methanol and the substantial metal loss observed in the isomerisation of sugars in either of the solvents [32] suggest that the extraction of tin from the materials is better aided by chelating functional groups of the substrate/product than by the acidity of the product. With respect to the stabilisation offered by the matrix in which tin is contained, our MFI zeolites appear strongly superior to bifunctional carbon-silica composites and BEA zeolites.[7c,8] Thus, in light of their performance and of the scalability of their synthesis, they stand as promising candidates for large-scale DHA isomerisation.

3.2 Process assessment

The results of the environmental assessment according to the CED metric are presented in Fig. 5a for the conventional technology and the various alternative hybrid process models of Table 1. The conventional enzymatic process (*LA-*) requires 109 MJ_{eq} to produce 1 kg of LA from GLU and the biggest environmental burden is created by the gate-to-gate energy utility consumption of the process. With respect to the alternative cascade processes, the single oxidative fermentation of pure GLY to DHA (*DHA-1*) was found to have a high environmental impact (102 MJ_{eq} kg_{LA}^{-1}) due to the large CED allocated to the raw material (35 MJ_{eq} kg_{LA}^{-1}). This evaluation was refined taking into account that, since crude GLY is a waste, its purification and use as a chemical feedstock effectively competes with its disposal, which is typically conducted *via* incineration or treatment in a waste water treatment plant. Because of the steam and electricity generated upon burning GLY, the CED value was slightly higher in the first case (108 MJ_{eq} kg_{LA}^{-1}, *DHA-2*), while preventing the consumption of energy and materials upon treatment in a waste water plant substantially reduced the CED value in the second case (65 MJ_{eq} kg_{LA}^{-1}, *DHA-3*). Hence, the most sustainable *DHA-3* model was selected for the assessment of the environmental footprint of the combined bio- and chemocatalytic process. In this respect, the effect of the type of catalyst and of its recyclability was studied besides the nature of the solvent. Accordingly, the use of MFI-AT (*LA-1*) was compared to that of Sn-MFI (*LA-2*), considering a lifetime of 3 catalytic runs in both cases. CED values of 121 and 114 MJ_{eq} kg_{LA}^{-1} were respectively obtained. The incomplete conversion of DHA over the tin-free catalyst penalises the process by 7 MJ_{eq} kg_{LA}^{-1} as it imposes additional unit operations to separate DHA from LA as well as to recover the butanol used in these steps. When the Sn-MFI zeolite was recycled for 7 instead of only 3 times, the CED value decreased by 11 MJ_{eq} kg_{LA}^{-1} due to the reduced materials consumption (*LA-3* and *LA-2,* respectively). Therefore, the reusability of the catalyst has a slightly higher impact than its activity (*i.e.*, DHA conversion) on the environmental footprint in the ranges herein investigated. It is worth noting that the latter process becomes competitive with respect to the traditional technology. When methanol was used as a medium for the DHA conversion (*LA-4*), the CED value of the cascade process was estimated at 96 MJ_{eq} kg_{LA}^{-1}, which is even moderately inferior to the case of GLU fermentation. The main reason for the alleviated environmental impact is the lower energy spent to recover methanol after reaction compared to the energy needed to concentrate the
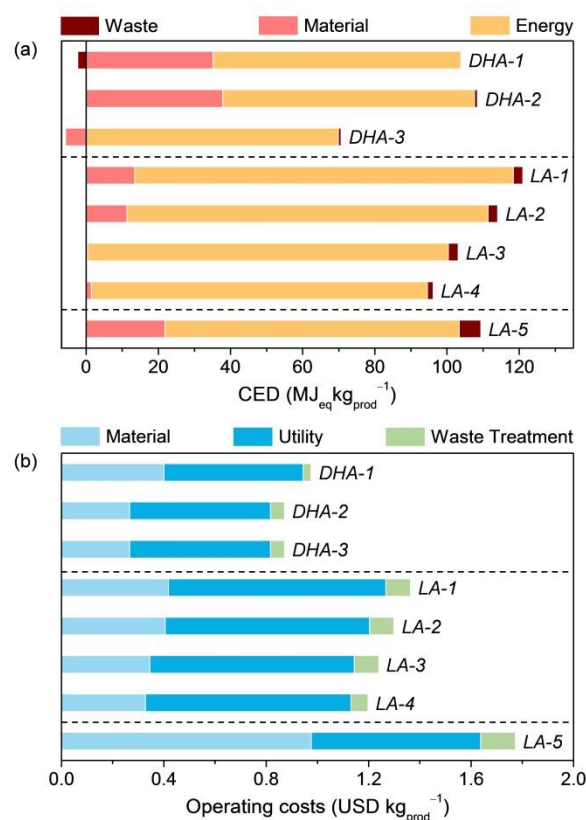

Fig. 5 (a) Cradle-to-gate LCA according to the non-renewable CED metric and (b) operating costs for various process layout scenarios.

aqueous reaction mixture through water evaporation. Similar overall trends were observed for the GWP and EI99 LCA metrics, which are presented and discussed in the ESI. It is expected that the assessment of LA production processes using MFI-ATSn would lead to equivalent results to the case of Sn-MFI in view of the identical performance and the virtually similar cost of preparation of the two catalysts.

The same process layouts and scenarios were evaluated in terms of operating costs as an economic metric. The results of this study are shown in Fig. 5b. The conventional LA production (*LA-5*) was found to have the highest operating cost with 1.77 USD kg_{LA}^{-1}. This originates from the higher price of GLU (400 USD ton^{-1}) compared to GLY (270 USD ton^{-1} for pure GLY and 110 USD ton^{-1} for crude GLY). Therefore, *ca.* 50% of the operating costs are allocated to the material in the conventional process. Considering the cascade bio- and chemocatalytic processes, the use of MFI-AT (*LA-1*) rather than Sn-MFI (*LA-2*) leads to a more costly technology (1.36 *versus* 1.30 USD kg_{LA}^{-1}, respectively, due to the more energy-intensive purification dictated by the incomplete conversion of DHA. The cascade process using the tin-containing catalyst becomes more economical by 0.06 USD kg_{LA}^{-1} upon its reuse for 7 times (1.24 USD kg_{LA}^{-1}, *LA-3*) as the material cost is contained. Based on these findings, it appears that a 12% higher LA yield produces the same impact as a doubled catalyst reusability on the operating costs. The production of LA through the methanol-based isomerisation (*LA-4*) is more economical by 3% than the best process performed in water resulting in 1.20 USD kg_{LA}^{-1}. This value is *ca.* one third smaller compared to the conventional LA

production. Finally, considering an LA price of 1800 USD ton^{-1},[23] the marginal profit of LA production *via* DHA isomerisation in methanol is 15 times higher than that of the conventional process (0.61 *versus* 0.04 USD kg$_{LA}$$^{-1}$).

Since utilising crude instead of pure GLY is one key factor for improving the economic and environmental performance of the bio/chemocatalytic process, a deeper investigation on the influence of the composition of crude glycerol (Table S6 in the ESI) on the assessment was performed. Accordingly, additional scenarios were evaluated in which the methanol and ash contents were separately increased at the expense of water, keeping the GLY and MONG contents constant. Furthermore, a limit case was considered in which the GLY content corresponds to the lowest value given in ref. [26], *i.e.*, 38 wt.%, and the difference to the standard amount was filled by an increase in methanol. In all cases, crude GLY disposal in waste water treatment plants was still considered as the more significant alternative option. The results of the assessment (Figs. S8-11 in the ESI) reveal that a higher ash or methanol content negligibly impacts the process with respect to both the environmental and economic footprint, while a low GLY-high methanol feedstock determines two interesting effects. Thus, the impact of treating the significantly larger process waste generated is counterbalanced by the avoided impact of treating a low GLY-high methanol stream, which ultimately ensures that the *LA-3* and *LA-4* processes remain environmentally more attractive than the conventional case (net CED values of 108 and 101 *versus* 109 MJ$_{eq}$ kg$_{LA}$$^{-1}$, Fig. S8). In contrast, since this compensating effect does not apply to the economic assessment, the operating costs are increased by *ca.* 30%. This implies a still less costly process than the enzymatic route, but a reduced margin profit-wise. It should be noted that in this sensitivity analysis it was assumed that the price of crude GLY does not to depend on its composition. Thus, as low-purity GLY will possibly have a lower price, the effective increase in operating costs should be more contained than in the current study. A more detailed discussion of these results can be found in the ESI.

3.3 Towards a continuous process

Since a continuous operation is widely preferred for the manufacture of bulk chemicals and would make the alternative LA production process even more advantageous, the possibility to extrapolate the catalytic systems herein studied for DHA isomerisation from a batch system to a continuous-flow reactor was explored. Only one contribution so far reports the attempt to produce LA and ML continuously.[33] Therein, a USY zeolite has been tested at 430 K and with a WHSV of 0.16 kg$_{DHA}$ kg$_{cat}$$^{-1}$ h^{-1} and has been found to rapidly deactivate in water but to retain *ca.* 90% of its activity after 48 h on stream in methanol. In our case (Fig. 6), Sn-MFI was evaluated under industrially more relevant conditions, *i.e.*, at a lower temperature (383 K) and a nearly 4-fold higher WHSV (0.60 kg$_{DHA}$ kg$_{cat}$$^{-1}$ h^{-1}). An ML yield of *ca.* 68% was observed in the first few hours of the test, which decreased by *ca.* 20% after 24 h. The apparently more limited stability of our tin-containing catalysts compared to the USY zeolite is likely due to an enhanced adsorption of C-based species (4 wt.% C in the used catalyst) due to the *ca.* 3 times more concentrated DHA solution. Since calcination was effective in restoring the initial catalyst properties (Fig. 4b), a strategy to
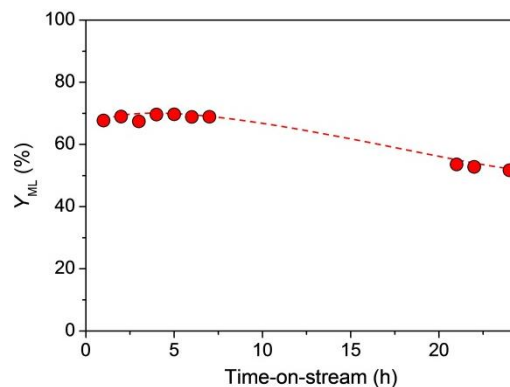

Fig. 6 ML yield during a continuous-flow experiment over Sn-MFI at 383 K.

enable a continuous LA production in the future could comprise the use of series fixed-bed reactors, alternatively in use/under regeneration.

4. Conclusions

Environmental, energetic and economic aspects of the currently applied enzymatic route for lactic acid production and of an alternative route comprising the biocatalytic oxidation of glycerol to dihydroxyacetone followed by chemocatalytic isomerisation have been herein evaluated by LCA using CED, EI99, GWP and operating costs as indicators. For the triose isomerisation step, the modelling was based on catalytic data herein gathered which uncover Sn-containing MFI zeolites prepared by either hydrothermal synthesis or alkaline-assisted stannation as outstandingly active, selective and reusable Lewis-acid catalysts.

The novel cascade process was shown to have substantially lower operating costs and a comparable till milder environmental and energetic footprint compared to the traditional technology. The economic aspects were found to be mainly determined by the costs associated with the raw materials and the sustainability to be critically influenced by both raw materials and process characteristics. In this respect, the high impact of the large CED of biodiesel-derived crude glycerol can be modulated taking into account the energy flows and material consumptions of the disposal procedures required if it is not used as a chemical feedstock. Additionally, considerable energy savings can be achieved employing a highly performing and recyclable Lewis-acid catalyst in the dihydroxyacetone isomerisation reaction. Accordingly, the Sn-containing MFI zeolites herein studied are preferable to Sn-free MFI zeolites previously reported. Interestingly, the one-step chemocatalytic manufacture of lactic acid in water is slightly energetically and economically more intensive than the two-step process based on methyl lactate production followed by hydrolysis due to the lower energy demands of the different downstream separation and purification procedures. Both process scenarios remain greener and economically more attractive than the conventional route even if the purity of the crude glycerol feedstock is as low as 38 wt.% .

Overall, the cascade bio-/chemocatalytic production of lactic acid from glycerol appears to have a strong potential for industrial implementation. In this direction, it is envisaged that the application of a continuous process for dihydroxyacetone isomerisation, which was herein demonstrated, and the possibility

of obtaining the triose intermediate from glycerol through a more productive chemocatalytic route, preferably also operated continuously, would render this alternative two-step process even more appealing.

Finally, this study emphasises the importance and potential of combining experimental results, rigorous process modelling and multi-criteria analysis for assessing the sustainability performance of proposed (bio)chemical production processes.

Acknowledgements

Notes and references

Institute for Chemical and Bioengineering, Department of Chemistry and Applied Biosciences, ETH Zurich, Vladimir-Prelog-Weg 1, CH-8093 Zurich, Switzerland.
E-mails: cecilia.mondelli@chem.ethz.ch; stavros.papadokonstantakis@chem.ethz.ch; jpr@chem.ethz.ch; Fax: +41 44 6331405; Tel: +41 44 6337120.

† Electronic Supplementary Information (ESI) available: Catalyst synthesis and characterisation methods; reusability tests of the catalysts in water and methanol and tin content in the solids after every run; X-ray diffraction and infrared spectroscopy of adsorbed pyridine of MFI-ATSn prior to and after LA production; process information for modelling the conventional biocatalytic LA production and the alternative chemocatalytic LA production from DHA; environmental assessment of the process models according to GWP and EI99; economic assessment of the process models according to profit calculations; background data for the environmental and economic assessment; See DOI: 10.1039/b000000x/

‡ These authors contributed equally to this work.

1 (a) A. Corma, S. Iborra, A. Velty, *Chem. Rev.*, 2007, **107**, 2411; (b) P. N. R. Vennestrøm, C. M. Osmundsen, C. H. Christensen, E. Taarning, *Angew. Chem., Int. Ed.*, 2011, **50**, 10502; (c) P. Y. Dapsens, C. Mondelli, J. Pérez-Ramírez, *ACS Catal.*, 2012, **2**, 1487.

2 (a) M. Dusselier, P. Van Wouwe, A. Dewaele, E. Makshina, B. F. Sels, *Energy Environ. Sci.*, 2013, **6**, 1415; (b) P. Mäki-Arvela, I. L. Simakova, T. Salmi, D. Yu. Murzin, *Chem. Rev.*, 2014, **114**, 1909.

3 (a) Available at www.foodproductiondaily.com/Packaging/PLA-bioplastics-production-could-hit-1m-tonnes-by-2020-nova-Institut, Retrieved May 2014; (b) Available at www.icis.com/resources/news/2012/04/30/9554300/big-potential-for-bioplastics-packaging, Retrieved May 2014

4 M. A. Abdel-Rahman, Y. Tashiro and K. Sonomoto, *Biotechnol. Adv.*, 2013, **31**, 877.

5 (a) C. B. Rasrendra, B. A. Fachri, I. G. B. N. Makertihartha, S. Adisasmito, H. J. Heeres, *ChemSusChem*, 2011, **4**, 768 (b) F. -F. Wang, C. -L. Liu, W. -S. Dong, *Green Chem.*, 2013, **15**, 2091 (c) Wang, W. Deng, B. Wang, Q. Zhang, X. Wan, Z. Tang, Y. Wang, C. Zhu, Z. Cao, G. Wang, H. Wan, *Nat. Commun.*, 2013, **4**, 2141.

6 E. Taarning, S. Saravanamurugan, M. S. Holm, J. Xiong, R. M. West, C. H. Christensen, *ChemSusChem*, 2009, **2**, 625.

7 (a) L. Li, C. Stroobants, K. Lin, P. A. Jacobs, B. F. Sels, P. P. Pescarmona, *Green Chem.*, 2011, **13**, 1175; (b) C. M. Osmundsen, M. S. Holm, S. Dahl, E. Taarning, *Proc. R. Soc. London, Ser. A*, 2012, **468**, 2000; (c) F. de Clippel, M. Dusselier, R. Van Rompaey, P. Vanelderen, J. Dijkmans, E. Makshina, L. Giebeler, S. Oswald, G. V. Baron, J. F. M. Denayer, P. P. Pescarmona, P. A. Jacobs, B. F. Sels, *J. Am. Chem. Soc.*, 2012, **134**, 10089.

8 Q. Guo, F. T. Fan, E. A. Pidko, W. N. P. van der Graaff, Z. C. Feng, C. Li, E. J. M. Hensen, *ChemSusChem*, 2013, **6**, 1352.

9 C. M. Lew, N. Rajabbeigi and M. Tsapatsis, *Microporous Mesoporous Mater.*, 2012, **153**, 55.

10 P. Y. Dapsens, C. Mondelli, J. Pérez-Ramírez, *ChemSusChem*, 2013, **6**, 831.

11 (a) C. Hammond, S. Conrad and I. Hermans, *Angew. Chem., Int. Ed.*, 2012, **51**, 11736; (b) J. Dijkmans, D. Gabriëls, M. Dusselier, F. de Clippel, P. Vanelderen, K. Houthoofd, A. Malfliet, Y. Pontikes and B. F. Sels, *Green Chem.*, 2013, **15**, 2777.

12 M. Taramasso, G. Perego, B. Notari, *US Patent* 4410501, 1983.

13 (a) J. Pérez-Ramírez, S. Mitchell, D. Verboekend, M. Milina, N. -L. Michels, F. Krumeich, N. Marti, M. Erdmann, *ChemCatChem*, 2011, **3**, 1731; (b) D. Verboekend, J. Pérez-Ramírez, *ChemSusChem*, 2014, **7**, 753.

14 (a) M. S. Holm, S. Saravanamurugan, E. Taarning, *Science*, 2010, **328**, 602; (b) R. K. Pazhavelikkakath Purushothaman, J. van Haveren, I. Melián-Cabrera, E. R. H. van Eck, H. J. Heeres, *ChemSusChem*, 2014, **7**, 1140; (c) H. J. Cho, C. Chang, W. Fan, *Green Chem.*, 2014, **16**, 3428; (d) L. Xu, H. Y. Zhang, Y. F. Zhao, B. Yu, S. Chen, Y. B. Li, L. D. Hao and Z. M. Liu, Green Chem., 2013, 15, 1520; (e) R. K. P. Purushothaman, J. van Haveren, D. S. van Es, I. Melián-Cabrera, J. D. Meeldijk, H. J. Heeres, Appl. Catal. B, 2014, 147, 92; (f) Y. Shen, S. Zhang, H. Li, Y. Ren, H. Liu, Chem. Eur. J., 2010, 16, 7368.

15 F. Yang, M. A. Hanna and R. Sun, *Biotechnol. Biofuels*, 2012, **5**, 13.

16 J. Svitel, E. Sturdik, *J. Ferment. Bioeng.*, 1994, **78**, 351.

17 (a) ISO 14040, European Committee for standardisation, 2006; (b) D. Kralisch, D. Ott, D. Gericke, *Green Chem*, 2015, DOI: 10.1039/C4GC01153H.

18 P. Y. Dapsens, C. Mondelli, B. T. Kusema, R. Verel, J. Pérez-Ramírez, *Green Chem.*, 2014, **16**, 1176.

19 N. K. Mal, V. Ramaswamy, P. R. Rajamohanan, A. V. Ramaswamy, *Microporous Mater.*, 1997, **12**, 331.

20 C. Rerat, S. Papadokonstantakis, K. Hungerbühler, *J. Air Waste Manage. Assoc.*, 2013, **63**, 349.

21 P. Dey, J. Sikder, S. Roy, P. Pal, *Clean Technol. Environ. Policy*, 2012, **14**, 827.

22 N. Thongchul, in *Bioprocessing Technologies in Biorefinery for Sustainable Production of Fuels, Chemicals, and Polymers*, eds. S-T. Yang, H. A. El-Henshay, N. Thongchul, John Wiley and Sons, New Jersey, 2013, ch. 16, pp. 293.

23 A. Bridgwater, R. Chinthappali, P. Smith, *Identification and market analysis of most promising added-value products to be co-produced with the fuels*, Aston University, 2010.

24 L. Nattrass, A. Higson, NNFCC, 2010.

25 D. T. Johnson, K. A. Taconi, *Environ. Prog.*, 2007, **26**, 338.

26 C. F. Hansen, A. Hernandez, B. P. Mullan, K. Moore, M. Trezona-Murray, R. H. King, J. R. Pluske, *Anim. Prod. Sci.*, 2009, **49**, 154.

27 G. Wernet, S. Conradt, H. P. Isenring, C. Jimenez-Gonzalez, K. Hungerbühler, 2010, *Int. J. LCA*, 1998, **15**, 294.

28 R. Frischknecht, R. Heijungs, P. Hofstetter, *Int. J. LCA*, 1998, **3**, 266.

29 B. Weidema, *J. Ind. Ecol.*, 2001, **4**, 11.

30 Ecoinvent Centre. 2010. Ecoinvent Data v2.2. Dübendorf, Switzerland: Swiss Center for Life Cycle Inventories.

31 Available at http://www.pall.com/pdfs/Fuels-and-Chemicals/FCBIODEN.pdf, Retrieved October 2014.

32 P. Y. Dapsens, J. Jagielski, C. Mondelli, J. Pérez-Ramírez, *Catal. Sci. Technol.*, 2014, **4**, 2302.

33 R. M. West, M. S. Holm, S. Saravanamurugan, J. Xiong, Z. Beversdorf, E. Taarning, C. H. Christensen, *J. Catal.*, 2010, **269**, 122.

Environmental and economic assessment of lactic acid production from glycerol using cascade bio- and chemocatalysis

Merten Morales,‡ Pierre Y. Dapsens,‡ Isabella Giovinazzo, Julia Witte, Cecilia Mondelli*, Stavros Papadokonstantakis*, Konrad Hungerbühler and Javier Pérez-Ramírez*

Institute for Chemical and Bioengineering, Department of Chemistry and Applied Biosciences, ETH Zurich, Vladimir-Prelog-Weg 1, CH-8093 Zurich, Switzerland. Fax: +41 44 6331405 Tel: +41 44 6337120; E-mails: cecilia.mondelli@chem.ethz.ch; stavros.papadokonstantakis@chem.ethz.ch; jpr@chem.ethz.ch.

1. Experimental

1.1. Catalyst synthesis and characterisation

Sn-MFI was synthesised according to the method reported elsewhere.[1] TEOS (93.7 g, Sigma-Aldrich, 98%) was mixed with a solution of $SnCl_4 \cdot 5H_2O$ (1.26 g, Sigma-Aldrich, 98%) in deionised H_2O (30 g) and allowed to react for 30 min under stirring. Then, TPAOH (198 g, Alfa Aesar, 20 wt.%) was added drop-wise and the mixture was stirred for another hour. Finally, 84 g of deionised H_2O were added and the solution was stirred for 30 min. The final molar ratio of the synthesis gel was 0.008 SnO_2:1 SiO_2:0.44 TPAOH:34.3 H_2O. The gel was transferred into a 500-cm^3 Teflon-lined autoclave, which was heated in an oven at 433 K for 3.5 days under static conditions. The obtained solid was recovered by filtration, washed thoroughly with deionised water, dried overnight at 338 K and finally calcined in static air at 823 K (heating rate: 5 K min^{-1}) for 5 h to ensure the complete removal of the organic structure-directing agent.

HSZ890 H0A (silicalite-1) was used for post-synthetic alkaline-assisted stannation.[2] The latter consisted of an alkaline treatment (AT) in an aqueous 0.3 M NaOH solution (15 cm^3 per gram of dried zeolite) containing 0.04 M of $SnSO_4$ (Acros, 98%) at 338 K for 30 min in an Easymax™ 102 reactor (Mettler Toledo). Due to the low solubility of the tin hydroxide formed, the solution was heated at 318 K for 1 h and filtered to remove the precipitate prior to the addition of the zeolite. The resulting modified metallosilicate (denoted as MFI-ATSn) was converted into its protonic form by three consecutive ion exchanges in aqueous 0.1 M NH_4NO_3 (6 h, 298 K, 100 cm^3 per gram of dried zeolite) and calcined as described above.

The carbon content in the used catalysts was determined by elemental analysis using a LECO CHN-9000 instrument. The content of Si and Sn in the solids and in the reaction mixtures was determined by inductively coupled plasma optical emission spectroscopy (ICP-OES) using a Horiba Ultra 2 instrument equipped with a photomultiplier tube detector. Prior to the measurements, the materials were digested in an acidic mixture ($HCl/HNO_3/HF$) under heating (343 K, overnight). Nitrogen sorption at 77 K was performed using a Quantachrome Quadrasorb-SI analyser on degassed samples (10^{-1} mbar, 573 K, 3 h). Powder X-ray diffraction (XRD) was conducted in a PANalytical X'Pert PRO-MPD diffractometer. Data were recorded in the 5-70° 2θ range with an angular step size of 0.05° and a counting time of 7 s per step. Fourier transform infrared (FTIR) spectroscopy of adsorbed pyridine was performed in a Bruker IFS 66 spectrometer equipped with a liquid N_2-cooled MCT detector. Self-supporting zeolite wafers (5 tons cm^{-2}, 20 mg, 1 cm^2) were pretreated at 10^{-3} mbar and 693 K for 4 h. After cooling down to room temperature, the samples were saturated with pyridine vapour (Sigma-Aldrich, >99.9%) and then evacuated at room temperature for 15 min and subsequently at 473 K for 30 min. Spectra were recorded in the 4000-650 cm^{-1} range at 4 cm^{-1} resolution by co-addition of 32 scans.
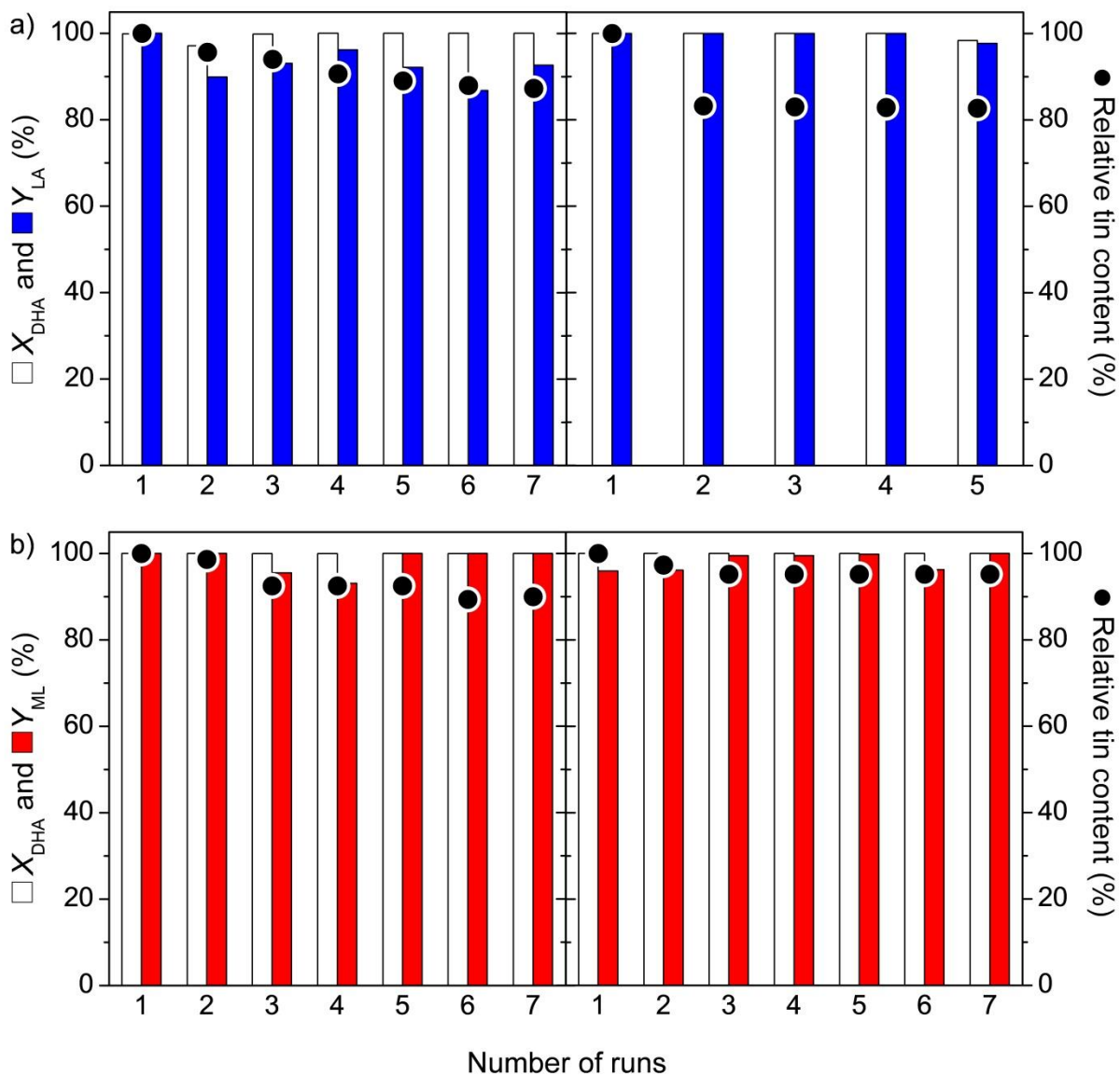
1.2. Catalyst recyclability

Fig. S1 Recyclability tests of the Sn-MFI (left panel) and MFI-ATSn (right panel) catalysts in (a) water and (b) methanol. The solids were calcined (823 K, 5 K min^{-1}, 5 h) prior to every reuse in order to remove the adsorbed by-products.
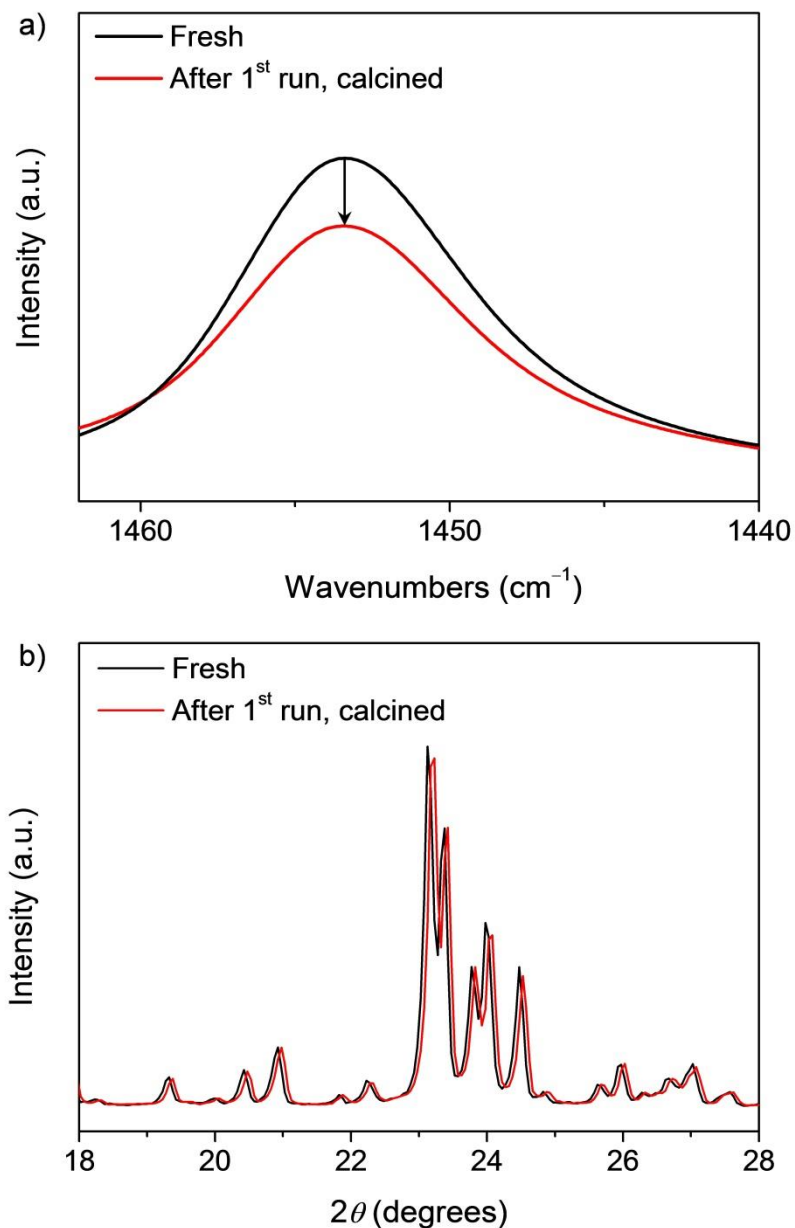
1.3. Catalyst characterisation

Fig. S2 (a) FTIR spectra of adsorbed pyridine and (b) XRD patterns of MFI-ATSn in fresh form and after one catalytic run in water. While the crystallinity of the zeolite was retained upon use, the concentration of Lewis-acid sites (calculated according to the method reported in [3]) decreased by 22%, which is in substantial agreement with the tin loss displayed in Fig. S1.

3

2. Process modelling

2.1. Biocatalytic LA production

The flowsheet generated for the conventional biocatalytic process for lactic acid (LA) production (*LA-5* model) is displayed in Fig. S3 and the relative life cycle inventory (LCI) data are shown in Table S1. The process comprises four main modelling steps: glucose (GLU) fermentation with *in situ* neutralisation of the as-formed LA with calcium hydroxide (Step-1), sulphuric acid-mediated hydrolysis of calcium lactate to LA (Step-2), esterification of LA to methyl lactate (ML) with recovery of the latter by distillation (Step-3) and hydrolysis of ML to recover pure LA (Step-4). Details to these steps are provided in the following.
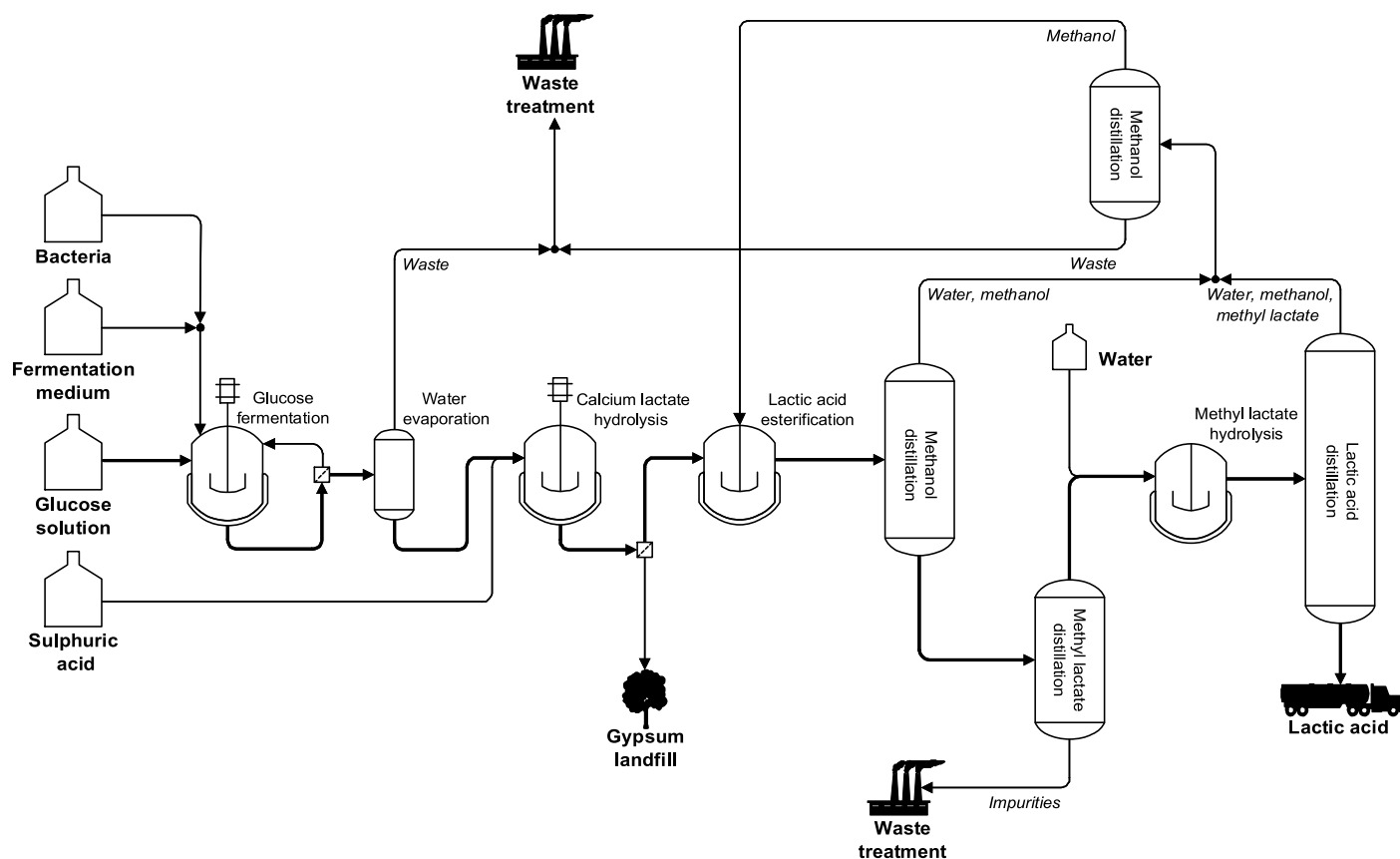
Fig. S3 Flowsheet for the LA production process from GLU according to the *LA-5* model.

Table S1 LCI data for the conventional biocatalytic LA production from GLU (*LA-5* model)

Material and energy	*LA-5* model	Units
Glucose	1.52	kg kg_{LA}^{-1}
Process water	14.8	kg kg_{LA}^{-1}
H_2SO_4	1.48	kg kg_{LA}^{-1}
Methanol	0.02	kg kg_{LA}^{-1}
Bacteria	0.01	kg kg_{LA}^{-1}
$Ca(OH)_2$	0.76	kg kg_{LA}^{-1}
Nutrients	0.07	kg kg_{LA}^{-1}
Steam (6bar)	52.1	kg kg_{LA}^{-1}
Cooling water	107	kg kg_{LA}^{-1}
Waste	16.7	kg kg_{LA}^{-1}
Gypsum	0.95	kg kg_{LA}^{-1}

### Step-1: GLU fermentation and in situ LA neutralisation

GLU fermentation and LA neutralisation were lumped in a single-step reaction:

$$C_6H_{12}O_6 + Ca(OH)_2 \longrightarrow [2(CH_3CHOCOO)^-]Ca^{2+} + 2H_2O$$

which was assumed to follow a pseudo power-law kinetics. The reaction was modelled using a RBATCH reactor in Aspen Plus® V8.2, considering a reaction time of 72 h, a temperature of 313 K, a pressure of 1 bar and a GLU conversion of 90%.[4] The input stream to the reactor had a composition of 84 wt.% water, 10 wt.% GLU, 5 wt.% calcium hydroxide and 1 wt.% nutrients. The LA bacteria (*lactobacillus*) content in the reactor was 4 wt.% with respect to the input stream.[5] Calcium hydroxide enabled to maintain the pH of the fermentation broth in the optimal range of 5.5-6.3 by converting LA to calcium lactate.[5,6]

Step-2: Sulphuric acid-mediated hydrolysis of calcium lactate

$$[2(CH_3CHOCOO)^-]Ca^{2+} + H_2SO_4 \longrightarrow 2CH_3CHOHCOOH + CaSO_4$$
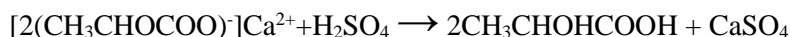
After flashing out most of the water, H_2SO_4 was injected (in an amount of twice the molar flow of calcium lactate) into the reactor to convert calcium lactate to LA by hydrolysis. This reaction was modelled with an RSTOIC reactor in Aspen Plus® V8.2, considering a reaction temperature of 403 K and a calcium lactate conversion of 90%.[7] A stoichiometric amount of $CaSO_4$ (*i.e.* gypsum) was formed in this transformation.[7] Owing to its relatively low solubility in water at 293 K (*ca.* 2.4 g L^{-1}),[8] it was assumed that 99 wt.% of the $CaSO_4$ can be separated through filtration. This gypsum is considered as a waste to be landfilled. This comprises the biggest disadvantage of the conventional LA production process.[9]

Step-3: Esterification of LA to ML and ML recovery by distillation

$$CH_3CHOHCOOH + CH_3OH \longrightarrow CH_3CHOHCOOCH_3 + H_2O$$
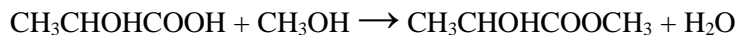
In order to separate LA from the other impurities formed in the fermentation process, an esterification with methanol was performed. In fact, thanks to the greater thermal stability of ML compared to LA, this avoids an energy-intensive and expensive vacuum distillation. This reaction was modelled with an RSTOIC reactor in Aspen Plus® V8.2, assuming a temperature of 353 K, a pressure of 1 bar, and a LA conversion of 88% and using a methanol input stream with 3 times the molar flow of that of LA.[10] After the esterification, water and methanol were first separated from ML, LA and impurities through distillation (DSTWU model in Aspen Plus® V8.2). In a second column (DSTWU model), ML was separated from impurities, which mainly comprised salts formed in the fermentation and LA that was not converted into ML. The waste stream of the second column was treated in a waste water treatment plant.

   Noteworthily, the conversion of LA to ML is usually carried out in a reactive distillation column. A rigorous RADFRAC model in Aspen Plus® V8.2 for such a reactive distillation would require experimental data for the reaction rates, which are not available in the literature. Therefore, this modelling step was simplified considering an RSTOIC reactor model and a DSTWU distillation model in Aspen Plus® V8.2 in series.

Step-4: Hydrolysis of ML to LA

$$CH_3CHOHCOOCH_3 + H_2O \longrightarrow CH_3CHOHCOOH + CH_3OH$$
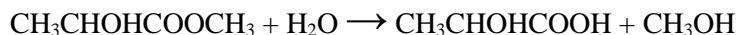
In this last step, ML was hydrolysed to LA in the presence of water and further purified by distillation. This reaction was modelled with a RSTOIC reactor in Aspen Plus® V8.2, considering a temperature of 353 K, assuming an ML

conversion of 95% and using a water input stream with 3 times the molar flow of ML.[7] LA was then separated from ML, water and methanol via a distillation column (DSTWU model in Aspen Plus® V8.2) operated at a pressure of 0.2 bar to ensure that the temperature of the reboiler does not exceed 453 K to prevent thermal degradation of LA. Under those conditions, LA was recovered with a purity of 99.99 wt.%.

Finally, methanol from Step-3 and Step-4 was recovered by distillation (DSTWU model) and recycled for the esterification of LA, whereas the outlet stream at the bottom of the column, containing mainly water, was directly sent to a waste water treatment plant.

2.2. Catalytic LA production from GLY-derived DHA

The alternative cascade process considered for the production of LA comprises the enzymatic conversion of glycerol (GLY) to DHA followed by its heterogeneously-catalysed isomerisation in water or isomerisation-esterification in methanol with subsequent hydrolysis. Environmental and economic aspects of this alternative route were studied, unravelling the impact of the type of solvent and the performance and recyclability of the catalyst used in DHA isomerisation. The latter comprised an alkaline-treated ZSM-5 zeolite,[11] denoted as MFI-AT, and the tin-containing MFI zeolites prepared by hydrothermal synthesis and alkaline-assisted stannation herein introduced, denoted as Sn-MFI and MFI-ATSn, respectively.

2.2.1. DHA production from GLY

For the DHA production from GLY, two process flowsheets were generated to account for the different purity of the GLY feedstock, which is either pure (99.99 wt.%, *DHA-1* model) or crude (various purities, see Table S6, *DHA-2* and *DHA-3* models).[12] The difference between the flowsheets is the presence of a pretreatment step for the removal of methanol, ash and matter organic non-glycerol (MONG) in the case of crude GLY to avoid potential GLY esterification in the DHA production steps. The flowsheet for the *DHA-2* and *DHA-3* models is shown in Fig. 1 of the main manuscript. This process can be divided into three main modelling steps: fermentation of GLY to DHA (Step-1), recovery of DHA through crystallisation out of butanol (Step-2) and recovery of butanol from the water-containing mother liquor through heterogeneous azeotropic distillation (Step-3). Details to these steps are provided below.

Step-1: Fermentation of GLY to DHA

The ash in the crude GLY was separated by conventional filtration (SSPLIT filter in Aspen Plus® V8.2). Since in 70% of the US biodiesel production sodium methylate represents the main constituent of the ash fraction, it was assumed that the ash only comprised this chemical species.[13] The crude GLY stream was then treated through flash evaporation (FLASH2 separator in Aspen Plus® V8.2) at 1 bar to remove most of the methanol and some of the water present. For the separation of MONG, a SEP separator in Aspen Plus® V8.2 could be applied. However, due to the lack of experimental data on the technology for the MONG separation from crude GLY, which is industrialised by PALL®,[14] this step was not modelled. The subsequent fermentation of GLY to DHA was modelled with an RBATCH reactor in Aspen Plus® V8.2, assuming a reaction time of 30 h, a temperature of 303 K, a pressure of 1 bar and a DHA conversion of 90%.[4] The input stream in the reactor had a composition of 89.5 wt.% water, 10 wt.%. GLY and 0.5 wt.% nutrients. The bacteria content in the reactor was 0.4 wt.% with respect to the input stream. Contrary to the fermentation of GLU to LA, no pH adjustment was required because the bacteria *gluconobacter oxydans* can stand pH values as low as 3.3.[15] GLY was completely converted into glyceric acid and DHA in a molar ratio of 0.028.[16] For the sake of simplicity, it was assumed that glyceric acid was the only by-product according to the following reaction scheme:

$$0.5O_2 + C_3H_8O_3 \longrightarrow C_3H_6O_3 + H_2O$$

6

$$O_2 + C_3H_8O_3 \longrightarrow C_3H_6O_4 + H_2O$$
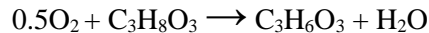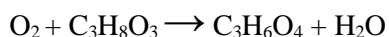
The fermentation broth was filtered and the bacteria were washed with water and recycled back into the fermenter. The liquid fraction was directed to the next flowsheet section for the recovery of DHA.

Step-2: Recovery of DHA through crystallisation out of butanol

The DHA recovery first comprised a flash evaporation (FLASH2 separator in Aspen Plus® V8.2) at 375 K and 1 bar for removing part of the water which is considered as a waste stream. Butanol was then added to the DHA-rich liquid stream in view of the relatively low solubility of DHA in this alcohol (*ca.* 6.3 g L^{-1} at 298 K) compared to water. After mixing, the stream was sent to a distillation column (DISTL column model in Aspen Plus® V8.2). In this separation step, a heterogeneous azeotropic mixture of water and butanol was removed from the top of the column while butanol with DHA and some glyceric acid impurities (< 1 wt.%) was recovered at the bottom of the column. The latter stream was treated in a crystalliser (CRYSTALLIZER solid model in Aspen Plus® V8.2) at 298 K where DHA precipitated. Glyceric acid remained in the mother liquor because its melting point is lower than 298K. DHA was separated from the mother liquor by filtration and directed to the LA production. The filtrate consisted of 95 wt.% butanol. Almost 99% of this butanol was recovered with a purity higher than 99.5 wt.% through a flash evaporation (FLASH2 separator in Aspen Plus® V8.2) that mainly removed the glyceric acid impurity. This was considered as a waste stream.

Along with the production of DHA to supply the LA manufacture, extra-pure DHA was produced for commercial use by implementing an additional unit in the process flowsheet. Thus, DHA was further washed (SWASH solid model in Aspen Plus® V8.2) with acetone and finally dried with air at 293 K (DRYER solid model in Aspen Plus® V8.2). The acetone stream leaving the washer was purified in a flash unit (FLASH2 separator in Aspen Plus® V8.2) and recycled (Fig. 1 in the main manuscript).

Step-3: Recovery of butanol from the water-containing mother liquor through heterogeneous azeotropic distillation

The heterogeneous butanol-water azeotrope (54 wt.% butanol and 46 wt.% water) was separated into an aqueous and an organic (*i.e.* butanol-rich) phase. The butanol-rich phase was recycled to the first column and the water-rich phase was directed to a second column. The remaining butanol was collected at the top of the latter unit in form of an azeotropic mixture, which was directed to a decanter while the resulting waste water was sent to a treatment plant. Almost all of the butanol could be recycled with this method of breaking the heterogeneous azeotrope. The make-up stream of fresh butanol was 0.61 kg h^{-1} and the butanol stream needed for the crystallisation 26.8 kg h^{-1}.

2.2.2. LA production from DHA in water

The DHA product stream was directed into the second part of the LA production, where DHA was converted into LA over zeolites. The flowsheet shown in Fig. S4 is based on the use of MFI-AT as the catalyst. Experimental data for this reaction have been presented elsewhere.[11] The flowsheet presented in Fig. 2a in the main manuscript considers tin-containing MFI catalysts, whose performance is reported in this paper. The structure of the two process flowsheets is similar. Firstly, DHA is converted into LA in a batch reactor (RBATCH reactor model in Aspen Plus® V8.2) and then LA is purified. LA production from DHA can be divided into three main modelling steps: the catalytic conversion of DHA into LA in water (Step-1), the recovery of the catalyst by filtration and regeneration *via* calcination (Step-2) and the separation of remaining impurities and DHA from LA by distillation and crystallisation with butanol in the model based on MFI-AT catalyst (Step-3a) or the recovery of LA through vacuum distillation in the model based on Sn-MFI catalyst (Step-3b). Details to these four steps are provided hereon.
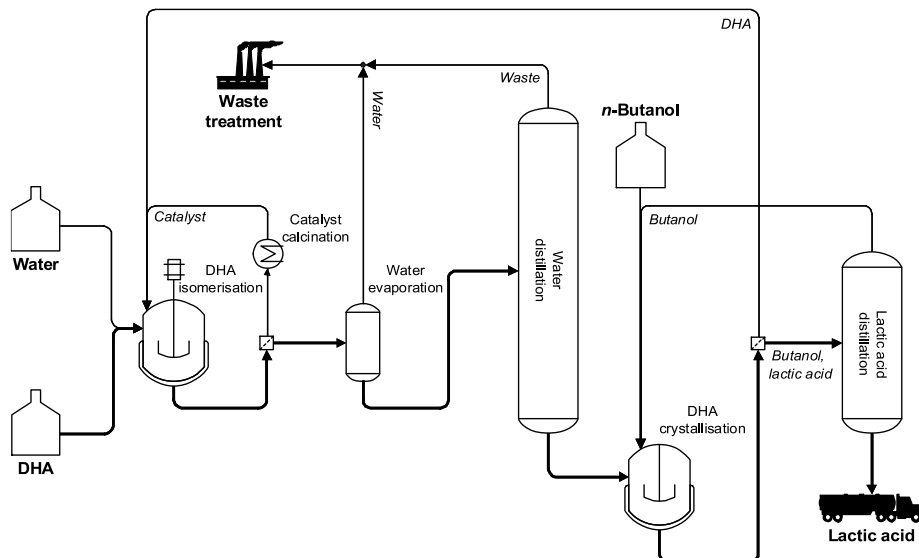
Fig. S4 Process flowsheet for the LA production from DHA with MFI-AT catalyst.

Step-1: Catalytic conversion of DHA to LA in water

In both flowsheets, the conversion of DHA into LA took place in a batch reactor modelled with an RBATCH model in Aspen Plus® V8.2. The inlet composition of the streams in the batch reactor is shown in Table S2 and the settings of the RBATCH model are summarised in Table S3.

Table S2 Composition of the mixture for the batch catalytic conversion of DHA into LA in water over the tin-free and the tin-containing catalyst
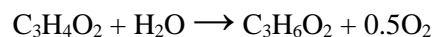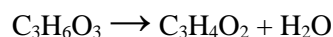
Inlet stream composition	MFI-AT model	Sn-MFI model	Units
DHA	15	15	wt.%
Catalyst	10	10	wt.%
Water	75	75	wt.%

Table S3 Settings for the batch reactor for the catalytic conversion of DHA into LA in water over the tin-free and the tin-containing catalyst

Reactor settings	MFI-AT model	Sn-MFI model	Units
Reaction time	6	1	h
Temperature	413	413	K
Pressure	4	4	bar
DHA conversion	90	100	%
LA yield	81	93	%
Catalyst recyclability	3	7	no. of runs

The DHA conversion and LA selectivity were 90 and 92% over MFI-AT[11] and 100 and 93% over Sn-MFI, respectively. Accordingly, a more energy-intensive purification of the outlet of the batch reactor was required in the first case. The Sn-MFI catalyst also exhibited a higher recyclability (7 runs) compared to the MFI-AT catalyst (3 runs).[11] While this parameter does not affects the purification steps, it leads to a larger catalyst consumption (the increased solid waste impact was not considered).

DHA was initially dehydrated into pyruvaldehyde, which was in turn transformed into LA, acetol and pyruvic acid. These steps are described by the following equations:

8

$$C_3H_6O_3 \longrightarrow C_3H_4O_2 + H_2O$$

$$C_3H_4O_2 + H_2O \longrightarrow C_3H_6O_3$$

$$C_3H_4O_2 + H_2O \longrightarrow C_3H_6O_2 + 0.5O_2$$

$$C_3H_4O_2 + 0.5O_2 \longrightarrow C_3H_4O_3$$

Step-2: Recovery of the catalyst by filtration and regeneration via calcination

The catalyst was separated from the reaction mixture by filtration and calcined at 823 K (5 K min^{-1}, 5 h) to remove the adsorbed by-products.

Step-3a: Recovery of LA through distillation and crystallisation (MFI-AT model)

After filtration, the stream was treated in a flash and a vacuum distillation unit (FLASH2 and DSTWU models in Aspen Plus® V8.2) to remove water and impurities. Thereafter, butanol was added to separate DHA from LA through crystallisation (CRYSTALLIZER model in Aspen Plus® V8.2) and filtration (SSPLIT model in Aspen Plus® V8.2). The DHA obtained was recycled back to the batch reactor. The LA-butanol mixture generated in this work-up was separated in a vacuum distillation unit (DSTWU model in Aspen Plus® V8.2).

Step-3b: Recovery of LA through distillation (Sn-MFI model)

The water content of the mixture was reduced by 60% using a flash evaporator operated at 375 K and 1 bar. The concentrated mixture underwent a vacuum distillation (DSTWU model in Aspen Plus® V8.2) which enabled to recover LA at the bottom of the column with a purity of 99.99 wt.% and water, acetol and pyruvic acid at the top of the column, which were sent to a waste water treatment plant. The column was operated at 0.04 bar to ensure that the temperature at the bottom of the column was below 453 K to prevent the thermal decomposition of LA.

2.2.3. LA production from DHA in methanol

In this case, DHA was isomerised in methanol to ML and LA was recovered by a subsequent hydrolysis step. The process flowsheet is shown in Fig. 2b in the main manuscript and can be divided into four main modelling steps: the catalytic conversion of DHA into ML in methanol (Step-1), the recovery of the catalyst by filtration and regeneration *via* calcination (Step-2), the recovery of LA through hydrolysis in a reactive distillation (Step-3) and the recovery of unreacted methanol by distillation (Step-4).

Step-1: Catalytic conversion of DHA to ML in methanol

The conversion of DHA to LA took place in a batch reactor (RBATCH model in Aspen Plus® V8.2). The inlet composition of the streams and the settings of the RBATCH model are shown in Tables S4 and S5, respectively.

Table S4 Batch reactor inlet composition for the catalytic conversion of DHA into LA in methanol over the tin-containing catalyst

Inlet stream composition	Sn-MFI model	Units
DHA	15	wt.%
Catalyst	10	wt.%
Methanol	75	wt.%

Table S5 Settings of the batch reactor for the catalytic conversion of DHA into LA in methanol over the tin-containing catalyst

Reactor settings	Sn-MFI model	Units
Batch time	2	h
Reactor temperature	413	K
Reactor pressure	11	bar
DHA conversion	100	%
ML yield	97	%
Catalyst recyclability	7	no. of runs

The experimental results for this reaction indicated that no by-product was formed. Thus, the reaction could be simply expressed as:
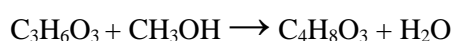
$$C_3H_6O_3 + CH_3OH \longrightarrow C_4H_8O_3 + H_2O$$

Step-2: Recovery of the catalyst by filtration and regeneration via calcination

The catalyst was separated from the reaction mixture by filtration and calcined at 823 K (5 K min^{-1}, 5 h) to remove the adsorbed by-products. The recyclability of the Sn-MFI catalyst was the same in the methanol and water environment, as shown in Tables S3 and S5.

Step-3: Recovery of LA through hydrolysis in a reactive distillation

The reaction mixture underwent a first distillation to separate ML from practically all the unreacted methanol (DSTWU model in Aspen Plus® V8.2). The ML leaving the bottom of the column is typically hydrolysed in a reactive distillation column. Due to the lack of experimental data and process information, this step was herein modelled combining an RSTOIC reactor and a DSTWU model in Aspen Plus® V8.2 in series. The reaction in RSTOIC took place at 353 K and 1 bar in the presence of added water. The molar ratio of ML to water in the inlet stream of the reactor was 1:3. The fractional conversion of ML was set to 0.95.[7] The mixture of methanol, ML, water and LA was directed to a distillation column, where practically all LA was recovered at the bottom with a purity of 99.99 wt.%. The column was operated at 0.1 bar to prevent the thermal decomposition of LA.

Step-4: Recovery of methanol

While all of the methanol present in the outlet stream of the batch reactor was recovered from the top of the first distillation column in Step-3 (purity 99.99 wt.%), further methanol was generated by the hydrolysis of ML (DSTWU model in Step-3) which needed to be recovered by separating it from water and traces of unhydrolised ML. This was performed in a distillation column (DSTWU model in Aspen Plus® V8.2) which enabled to obtain 99.9% of the methanol at a purity of 99.98 wt.%. The methanol recovered from both columns was recycled back to the batch reactor for the conversion of DHA into ML. The waste stream, leaving the bottom of this last column was sent to a waste water treatment plant.

3. Process assessment

The production of LA through the alternative cascade process from crude GLY was first evaluated using a standard GLY composition (Table S6) selected based on the study of Hansen *et al*.[12] In particular, this composition was calculated averaging the data reported for each fraction in Table 2 of the mentioned article, excluding the entry relative to a GLY feedstock of exceptionally low quality (*i.e*., 38.4 wt.%). In addition, other three GLY compositions were

considered (Table S6). In the high ash and high methanol cases, the ash or methanol content was increased by an amount corresponding to the water fraction, which was simultaneously set to zero. Noteworthy, the depletion of the water content in these scenarios implies a higher resource consumption of process water, since the inlet concentration of GLY in the fermentation unit should not exceed 10 wt.%. Furthermore, while the lack of water would suggest a more convenient alternative disposal of the crude GLY in an incineration unit, our comparative situation remained the disposal in a waste water treatment plant. Indeed, the analysis of these non-realistic GLY compositions was only meant to unravel the impact of the purification of single components on the overall process sustainability, which was still contrasted to the most representative alternative disposal strategy. The low GLY composition was generated considering the GLY content in the feedstock neglected in the calculation of the standard composition, maintaining the water, ash and MONG contents of the standard case and defining an amount of methanol sufficient to close the balance to 100%.

Table S6 Inlet compositions of crude GLY considered in the study of the alternative cascade process

	Standard	High ash	High methanol	Low GLY	Units
GLY	75.84	75.84	75.84	38.40	wt.%
Water	5.98	0	0	5.98	wt.%
Ash	5.32	11.30	5.32	5.32	wt.%
Methanol	3.29	3.29	9.27	40.73	wt.%
MONG	9.57	9.57	9.57	9.57	wt.%

3.1. Standard GLY composition

3.1.1. Global warming potential

The global warming potential (GWP) values (Fig. S5) show similar trends to the CED results presented and discussed in the main manuscript. More specifically, the data indicate that the conventional process (*LA-5* model) emits into the environment 7.6 kg of CO_2 per kg of LA. For the alternative process, the highest environmental burden is the production of DHA from pure GLY. Indeed, the GWP for the *DHA-1* model alone is 7.1 kg_{CO2-eq} kg_{DHA}^{-1}. The production of DHA from crude GLY has at least a 30% lower impact than its production from pure GLY if the alternative utilisation scenario for GLY is burning in an incineration plant, recovering the respective steam and/or electricity (*DHA-2* model). If crude GLY is considered as a waste to be treated in a waste water treatment plant, the
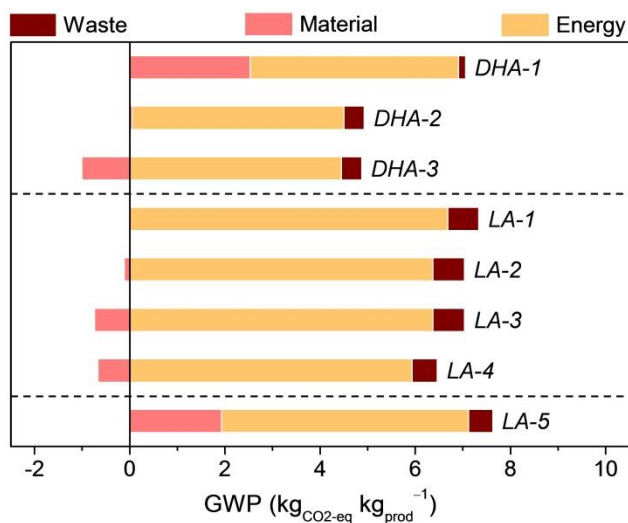

Fig. S5 Cradle-to-gate LCA according to the GWP-100a metric for various process scenarios.

GWP value becomes even smaller (3.9 kg_{CO2-eq} kg_{DHA}^{-1}, *DHA-2* model). The cascade LA production process using the MFI-AT catalyst (*LA-1* model) has a GWP value of 7.3 kg_{CO2-eq} kg_{LA}^{-1}. When the Sn-MFI catalyst is employed (*LA-2* model), the environmental impact is reduced to 6.9 kg_{CO2-eq} kg_{LA}^{-1} since the full DHA conversion and extremely high LA selectivity in this case enable a less energy-intensive purification of the LA stream. The lowest environmental impact (5.8 kg_{CO2-eq} kg_{LA}^{-1}) can be reached when the conversion of DHA into LA is performed in methanol (*LA-4* model). In this best-case scenario, the improvement of the GWP value is 24% compared to the conventional method (*LA-5* model).

3.1.2. Eco-Indicator 99

The trends of the Eco-Indicator 99 (EI99) values (Fig. S6) are similar to the CED and GWP cases, although larger variations are observed. In particular, the results show that the conventional design (*LA-5* model) has an environmental impact of 0.53 points kg_{LA}^{-1}. In relation to the DHA production from GLY, the environmental impact is the highest if pure GLY is used (1.09 points kg_{DHA}^{-1}, *DHA-1* model), because of the strong contribution of this feedstock to the material impact. This value can be reduced to 0.38 or 0.26 points kg_{DHA}^{-1} if crude GLY is considered as a waste to be treated in an incineration or waste water treatment plant, respectively. Accordingly, a decrease of the environmental footprint of even 65% can be determined for the biocatalytic step of the DHA production. The cascade *LA-4* process leads to an environmental impact for LA production of 0.39 points kg_{LA}^{-1}, which represents a reduction of 26% compared to the conventional technology (*LA-5* model). The impact of the materials on the LA production according to the EI99 indicator is not negative as in the case of the GWP metric (Fig. S5). The reason is that the catalyst has a higher impact for the EI99 compared to the GWP indicator.
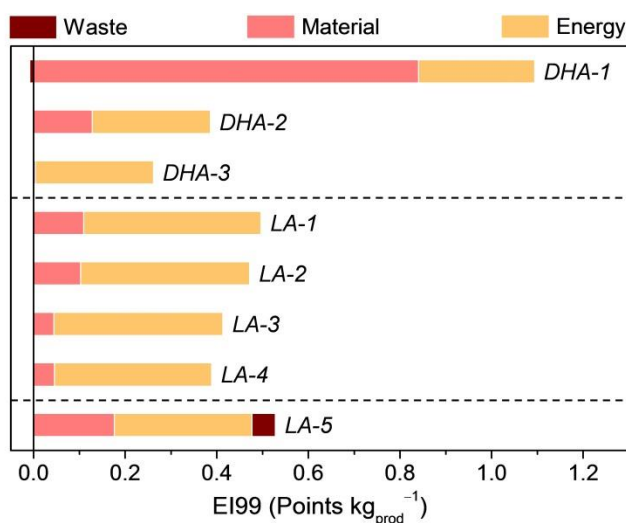

Fig. S6 Cradle-to-gate LCA according to the EI99 metric for various process scenarios.

3.1.3. Economic assessment

The results of the economic assessment are shown in Fig. S7. The currently practiced GLU fermentation process (*LA-5* model) gives a profit of only 0.04 USD kg_{LA}^{-1} due to the high operating costs. The highest profit with respect to GLY utilisation would be reached if DHA was considered as the end-product. For instance, assuming the *DHA-3* model, no competition for the utilisation of GLY with other markets (*i.e.* crude GLY is considered as a waste) and a market price of DHA of 4700 USD ton^{-1}[17], a profit of 3.8 USD kg_{LA}^{-1} could be obtained. Still, it has to be kept in mind that the market for DHA is rather small and easy to saturate,[17] Indeed, one strong motivation for its further processing to LA
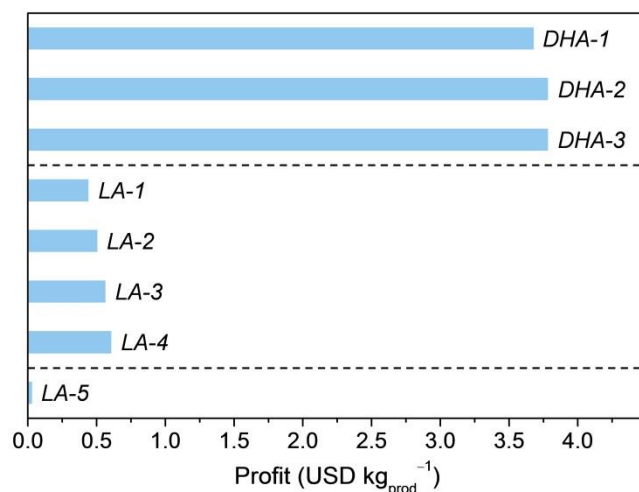
Fig. S7 Profit for various process scenarios.

is the much bigger market of the latter. The *LA-4* model has the highest profit (0.6 USD kg$_{LA}$), which is 15 times greater than for the current enzymatic route. All profit calculations mentioned above did not include the respective investment expenditure.

3.2. Other GLY compositions

3.2.1. Cumulative energy demand

The CED values determined for the alternative processes using GLY with non-standard composition are depicted in Fig. S8. Due to the low additional energy input for the purification of the GLY feedstock and for the waste water treatment, only a minor effect on the overall environmental impact was observed for the high ash and high methanol scenarios. A stronger variation was found for the low GLY case. Indeed, while the high concentration of methanol of this crude feedstock negligibly affects the energy required in the process, it leads to a more demanding waste treatment. Still, since the use of crude GLY as a chemical feedstock enables to save equivalent materials and energy input by avoiding its disposal, the overall CED values for the low GLY scenario remain very close to those determined for the standard GLY composition scenario. This outcome makes us confident that the non-quantifiable impact due to the MONG removal shall not compromise the meaningfulness of our analysis. The results of the assessment of the *LA-4* process using standard and low-quality GLY are detailed in Table S7.

Table S7 Cradle-to-gate LCA according to the non-renewable CED metric for the *LA-4* process scenarios based on the standard and low crude GLY compositions

	Standard	Low GLY	Units
Material	1.45	-19.34	MJ$_{eq}$ kg$_{prod}^{-1}$
Energy	93.12	97.82	MJ$_{eq}$ kg$_{prod}^{-1}$
Waste	1.57	22.31	MJ$_{eq}$ kg$_{prod}^{-1}$
Total	96.13	100.79	MJ$_{eq}$ kg$_{prod}^{-1}$

Fig. S8 Cradle-to-gate LCA according to the non-renewable CED metric for the (a) high ash, (b) high methanol and (c) low GLY scenarios.

3.2.2. Global warming potential

The trends in the GWP values for the high ash and high methanol scenarios resemble those of the CED values. In the low GLY case, the waste determines a strong increase in the environmental footprint but this is counterbalanced by the reduced impact of the materials which is due to the utilisation of waste GLY as a raw material.
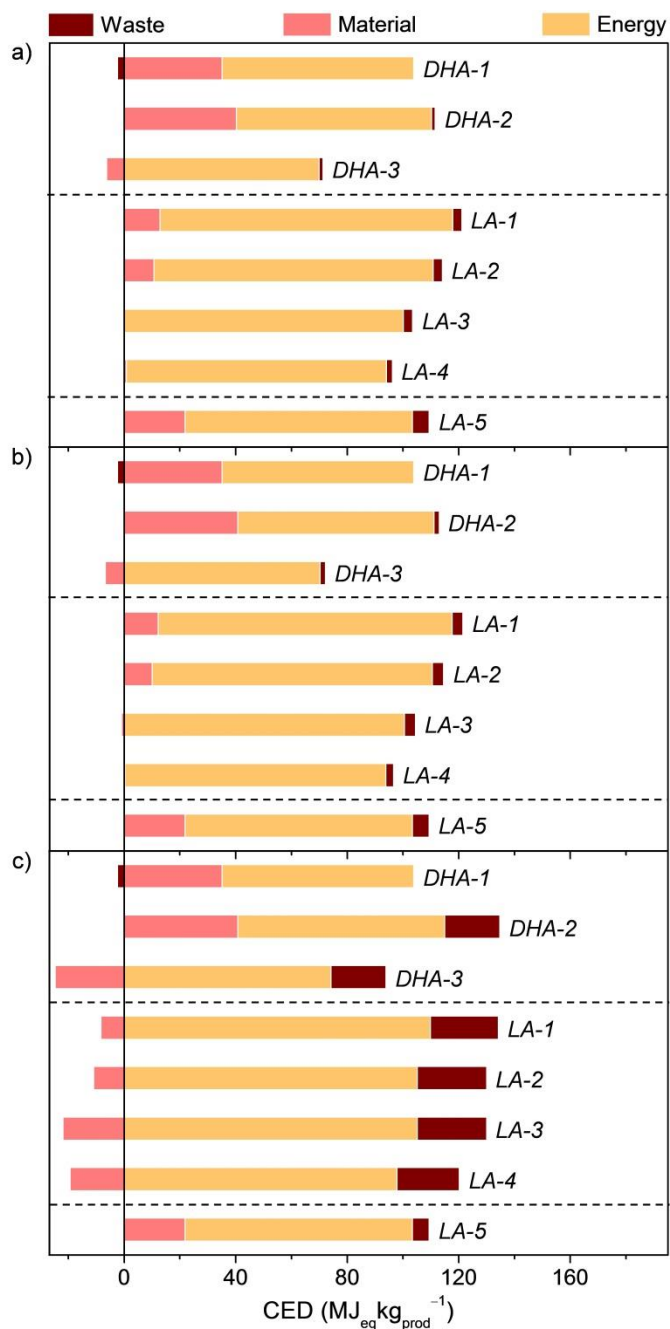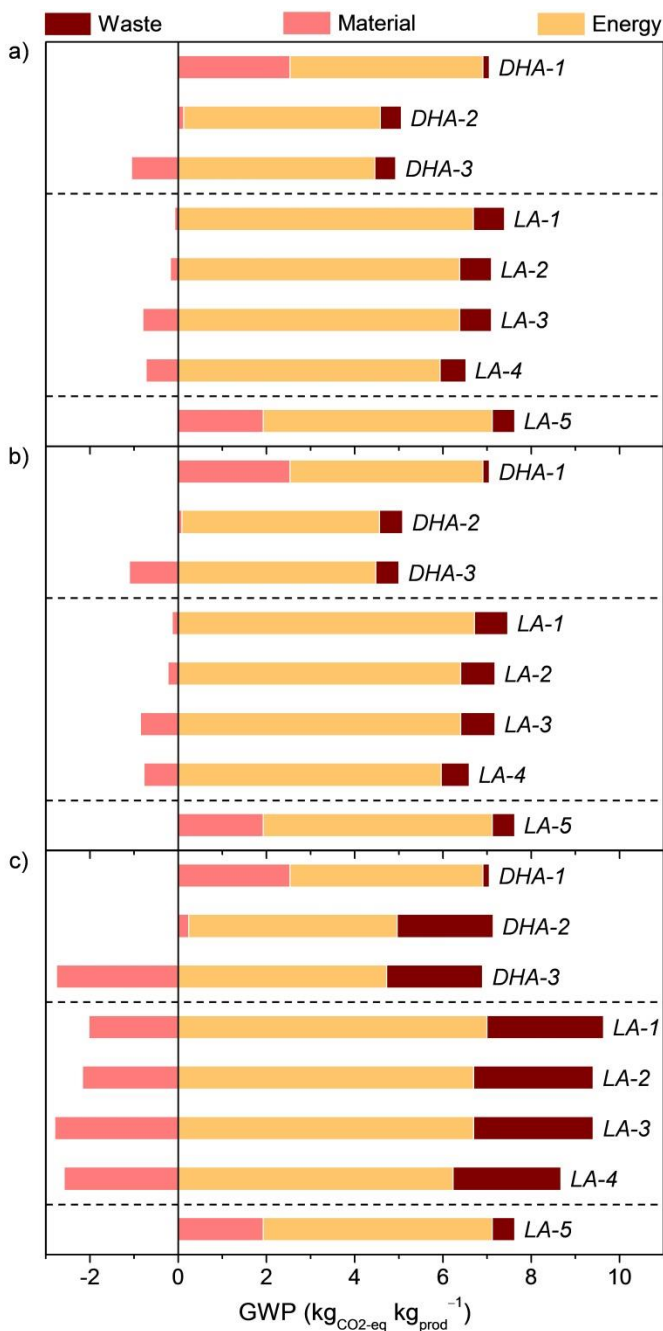

Fig. S9 Cradle-to-gate LCA according to the non-renewable GWP metric for the (a) high ash, (b) high methanol and (c) low GLY scenarios.

3.2.3. Eco-Indicator 99

The process assessment results according to the EI99 metric are in line with those based on the CED and GWP indicators for the high ash and high methanol cases. For the low GLY scenario, the impact for the material in *LA-3* and *LA-4* vanishes. This is an effect of the reduced influence of the catalyst due to its high recyclability in these processes.
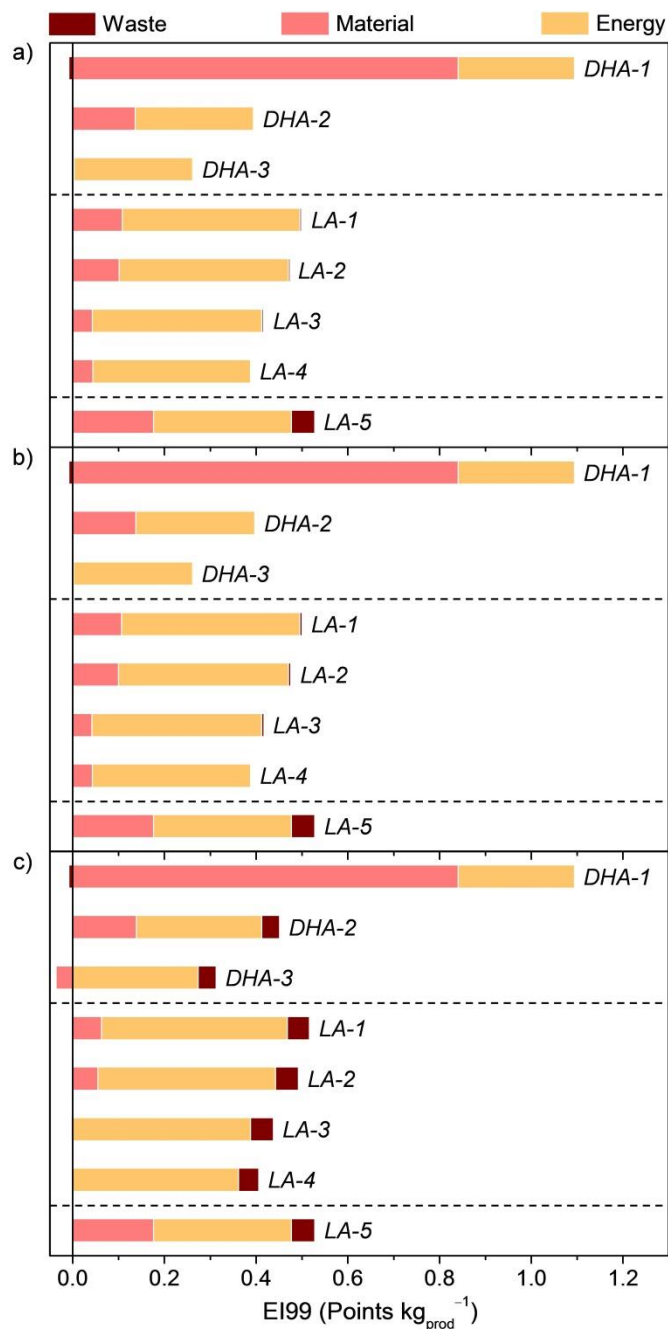

Fig. S10 Cradle-to-gate LCA according to the non-renewable EI99 metric for the (a) high ash, (b) high methanol and (c) low GLY scenarios.

3.2.4. Economic assessments

The results for the economic assessment of the processes using non-standard GLY compositions are shown in Fig. S11. Only minor variations in operating costs and profit compared to the standard scenario are detected for the high ash and high methanol situations. This is a consequence of a limited increase in the costs associated with the raw material pretreatment and the process waste treatment. In contrast, the use of a low-quality feedstock (low GLY case) leads to a significant increase in operating costs (36% for the *LA-4* model) since, due to the low concentration of GLY, a higher amount of crude GLY needs to be purchased to match the LA production in the standard scenario and a higher amount of methanol has to be treated in a waste water treatment plant. Still, it should be underlined that even in this case the profit of the alternative cascade process *LA-4* is 5 times higher than that of the conventional technology *LA-5*. Since it was assumed that the price of crude GLY does not to depend on its composition, but a low-purity GLY will realistically have a lower price, the profit of the alternative process might remain more considerable even when a low-quality GLY feedstock is employed.
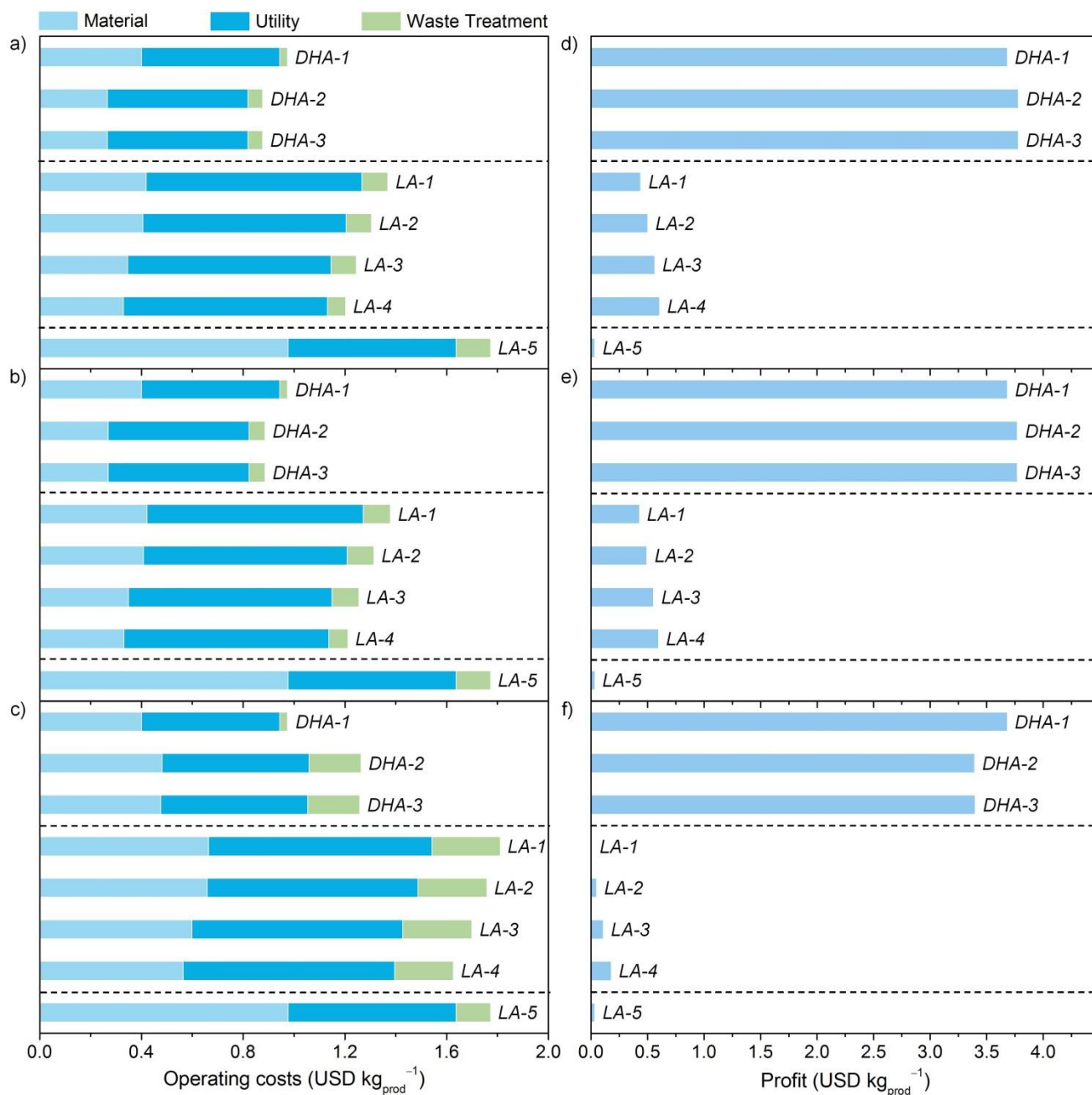
Fig. S11 Operating costs for the (a) high ash, (b) high methanol and (c) low GLY scenarios. Profit for the (d) high ash, (e) high methanol and (f) low GLY scenarios.

3.3. Background data for the environmental and economic assessment

The background data used in this study for the environmental and economic assessment with respect to the consumption of resources are presented in Table S8, while those related to the environmental impact of the process emissions (*i.e.,* those generated by the incineration units or waste water treatment plants, as no other direct process emissions are considered in this study) are presented in Table S9.

Table S8 Background data for the environmental (without renewable resources) and economic assessment with respect to resources consumption (Source: Ecoinvent database, www.alibaba.com and refs. [17,18])

Substance	CED (MJ$_{eq}$ kg^{-1})	EI99 (Points kg^{-1})	GWP (kg$_{CO2-eq}$ kg^{-1})	Price (USD ton^{-1})
Process water	2.79e-04	1.83e-06	2.45e-05	1
Ammonium sulphate	44.4	0.21	2.69	160
Diammonium phosphate	56.4	0.28	2.80	800
Glucose from sugar beet	6.49	0.05	0.51	400
Sulphuric acid	2.02	0.04	0.12	150
Methanol	37.4	0.13	0.74	348
Calcium hydroxide	5.50	0.03	0.99	100
Bacteria	18.6	0.08	1.04	1000
GLY	23.9	0.73	1.99	270
Butanol	80.4	0.29	2.60	822
Acetone	46.2	0.17	1.18	685
Zeolites	73.7	0.39	4.20	400
Crude GLY - INC	-18.3	-0.06	0.32	111
Crude GLY - WWTP	113	0.24	10.4	111
Steam (6bar)	1.56	0.01	0.10	20
Electricity (MU kWh^{-1})	9.87	0.02	0.49	0.10
Cooling water from river	0.00	0.00	0.00	0.15
Natural gas	1.24	4.03e-03	1.22e-02	600
Sodium hydroxide 30 wt.%	22.8	6.26e-02	1.09	570
Hydrochloric acid 32 wt.%	17.5	0.060	0.853	190
Polydimethylsiloxane	62.7	0.22	2.71	1000
Iron(III) chloride 40 wt.%	16.3	6.35e-02	0.803	360
Calcium chloride	11.0	5.18e-02	0.854	440
Gypsum landfill	0.65	4.22e-02	1.34e-02	4.81e-05

Table S9 Background data for the environmental impact for the emissions (Source: Ecoinvent database and ref. [18])[a]

Substance	EI99 (Points kg^{-1})	GWP (kg$_{CO2-eq}$ kg^{-1})
Carbon dioxide	5.46e-02	1
Carbon monoxide	8.36e-02	-
Nitrogen dioxide	2.75	1.57
Particles	9.74	-
Ammonia	3.42	-

[a] Gypsum emissions are presented in Table S6.

3.4 Calculation of the environmental indicators

The LCA calculations for the flowsheets were performed based on the background data collected in Tables S8 and S9. Tables S10 and S11 show the calculations for LA production according to the conventional technology (*LA-5* model) and the most promising alternative cascade process (*LA-4* model) applying the standard crude GLY composition.

Table S10 LCA calculations for LA production *via* the conventional process

	Material								Energy			Waste	
	Water	Sulphate	Phosphate	Glucose	Sulphuric acid	Methanol	Calcium hydroxide	Bacteria	Steam (6bar)	Cooling water	Electricity	WWTP	Gypsum landfill
Flow (kg h^{-1})	166	0.42	0.42	17	17	0.25	8.45	0.13	585	12036	1.10E-03 [a]	188	10.63
CED (MJ$_{eq}$ h^{-1})[b]	0.05	18	24	111	33	9.35	46	2.42	914	0	1.09E-02	60	6.94
EI99 (Points h^{-1})[b]	0	0.09	0.12	0.86	0.64	0.03	0.22	0.01	3.37	0	2.52E-05	0.13	0.45
GWP (kg$_{CO2eq}$ h^{-1})[b]	0	1.13	1.18	8.65	2.01	0.19	8.33	0.14	58	0	5.36E-04	5.55	0.14
$\sum$CED (MJ$_{eq}$ h^{-1})[c]	245								915			67	
$\sum$EI99 (Points h^{-1})[c]	1.97								3.37			0.58	
$\sum$GWP (kg$_{CO2eq}$ h^{-1})[c]	22								58			5.69	
CED (MJ$_{eq}$ kg^{-1})[d]	21.83								81.52			5.99	
EI99 (Points kg^{-1})[d]	0.18								0.30			0.05	
GWP (kg$_{CO2eq}$ kg^{-1})[d]	1.93								5.19			0.51	

CED$_{Process}$ (MJ$_{eq}$ kg^{-1})[e]	109
EI99$_{Process}$ (Points kg^{-1})[e]	0.53
GWP$_{Process}$ (kg$_{CO2-eq}$ kg^{-1})[e]	7.63

[a] Flow (kW)

[b] Obtained by multiplying the flow with the background data in Tables S8 and S9

[c] Summation of CED/EI99/GWP values for material, energy and waste

[d] Summation of CED/EI99/GWP values for material, energy and waste divided by the LA productivity calculated for this process (11.22 kg h^{-1})

[e] Summation of CED/EI99/GWP values of material, energy and waste

Table S11 LCA calculations for LA production from crude GLY *via* the alternative cascade *LA-4* process

	Material								Energy			Waste	
	Water	Crude GLY	Sulphate	Phosphate	Butanol	Zeolites	Bacteria	Methanol	Steam (6bar)	Cooling Water	Electricity	WWTP	INC
Flow (kg h^{-1})	102	12.87	0.27	0.27	0.61	0.92	0.01	0.27	527	13672	0	108	1.26
CED (MJ$_{eq}$ h^{-1})^b	0.03	-115	11.93	15.11	49.29	68	0.15	10.19	823.62	0	0	18.59	-31
EI99 (Points h^{-1})^b	0	-0.25	0.06	0.08	0.18	0.36	0	0.03	3.04	0	0	0.04	-0.1
GWP (kg$_{CO2eq}$ h^{-1})^b	0	-10.64	0.72	0.75	1.59	3.87	0.01	0.20	52	0	0	1.71	0.55
$\sum$CED (MJ$_{eq}$ h^{-1})^c	39.09								823			-12.40	
$\sum$EI99 (Points h^{-1})^c	0.46								3.04			-0.06	
$\sum$ GWP (kg$_{CO2eq}$ h^{-1})^c	-3.50								52.47			2.26	
CED (MJ$_{eq}$ kg^{-1})^d	4.42								93.05			-1.40	
EI99 (Points kg^{-1})^d	0.05								0.34			-0.01	
GWP (kg$_{CO2eq}$ kg^{-1})^d	-0.40								5.93			0.26	
CED$_{Process}$ (MJ$_{eq}$ kg^{-1})^e					96								
EI99$_{Process}$ (Points kg^{-1})^e					0.39								
GWP$_{Process}$ (kg$_{CO2-eq}$ kg^{-1})^e					5.79								

^{a} Flow (kW)

^{b} Obtained by multiplying the flow with the background data in Tables S8 and S9

^{c} Summation of CED/EI99/GWP values for material, energy and waste

^{d} Summation of CED/EI99/GWP values for material, energy and waste divided by the LA productivity calculated for this process (8.85 kg h^{-1})

^{e} Summation of CED/EI99/GWP values of material, energy and waste

References

[1]   N. K. Mal, V. Ramaswamy, P. R. Rajamohanan and A. V. Ramaswamy, *Microporous Mater.*, 1997, **12**, 331.

[2]   P. Y. Dapsens, C. Mondelli, B. T. Kusema, R. Verel and J. Pérez-Ramírez, *Green Chem.*, 2014, **16**, 1176.

[3]   C. A. Emeis, *J. Catal.*, 1993, **141**, 347.

[4]   R. Datta and M. Henry, *J. Chem. Technol. Biotechnol.*, 2006, **81**, 1119.

[5]   P. Dey, J. Sikder, S. Roy and P. Pal, *Clean Technol. Environ. Policy*, 2012, **14**, 827.

[6]   N. Thongchul, in *Bioprocessing Technologies in Biorefinery for Sustainable Production of Fuels, Chemicals, and Polymers,* S.-T. Yang, H. A. El-Henshay and N. Thongchul Eds., John Wiley and Sons, New Jersey, 2013, Chapter 16, p. 293.

[7]   M. Cockrem and P. Johnson, *US Patent* 5210296, 1993.

[8]   Available at www.echa.europa.eu, retrieved on 24.06.2014.

[9]   S. C. Prescott and C. G. Dunn, *Industrial Microbiology*, McGraw Hill, New York, 1959, p. 304.

[10]   X. Sun, Q. Wang, W. Zhao, H. Ma and K. Sakata, *Sep. Purif. Technol.*, 2006, **49**, 43.

[11]   P. Y. Dapsens, C. Mondelli and J. Pérez-Ramírez, *ChemSusChem*, 2013, **6**, 831.

[12]   C. F. Hansen, A. Hernandez, B. P. Mullan, K. Moore, M. Trezona-Murray, R. H. Kingand and J. R. Pluske, *Anim. Prod. Sci.*, 2009, **49**, 154.

[13]   P. Thane, *biofuels international*, 2008, **2**, 53

[14]   Available at www.pall.com/pdfs/Fuels-and.../FCBIODEN.pdf, Retrieved at October 2014

[15]   W. Charney, *US Patent* 4076589, 1987.

[16]   J. Svitel and E. Sturdik, *J. Ferment. Bioeng.*, 1994, **87**, 351.

[17]   A. Bridgwater, R. Chinthappali and P. Smith, *Identification and market analysis of most promising added-value products to be co-produced with the fuels*, Aston University, 2010.

[18]   C. Rerat, S. Papadokonstantakis and K. Hungerbühler, *J. Air Waste Manage. Assoc.*, 2013, 349.